

**People's Democratic Republic of Algeria**  
**Ministry of Higher Education and Scientific Research**  
**University M'HAMED BOUGARA – Boumerdes**



**Institute of Electrical and Electronic Engineering**  
**Department of Electronics**

Final Year Project Report Presented in Partial Fulfilment of the  
Requirements for the Degree of

**MASTER**

**In Telecommunication**

**Option: Telecommunications**

Title:

**Design and Analysis of a Miniaturized  
Microstrip Yagi-Uda Antenna**

Presented by:

- **BENDAIMI Amira**

Supervisor:

**Pr. A. AZRAR**

Registration Number:...../2021

## Acknowledgements

First and foremost, I would like to thank Almighty ALLAH for giving me the courage and the strength to complete this dissertation successfully, despite all the difficulties,

*Alhamdulillah.*

My sincere appreciations goes to my supervisor and principal lecturer “**Pr. Arab AZRAR**”, who has followed this work with great interest , I would like to express my deep respect and gratitude toward his presence despite all the responsibilities and duties that rest on his shoulders, his support, patience and precious orientation as well

It was a great honor to work under his guidance; without his professional advices, insightful criticisms and careful editing this work would never be in this form.

***Thank you for this worthwhile experience!***

I would like to take this opportunity to thank **ALMITECH** team especially **Riyad** and **Riyan** for the time, the facilities and the special service that have provided me during the fabrication of the proposed antennas

Last and not least, may all people who helped me throughout this journey, find here an expressions of my deep gratitude



# DEDICATION

This work is wholeheartedly dedicated to my beloved parents, who have been my source of strength, hope and motivation. Thank you mom and dad for your unconditional support and courage in all the path of my studies.

I dedicate this work to all my family especially my brothers: **Djamel, Amine** and **Hawasse** who are certainly proud of their little sister, I am lucky to have you in my life! And to my dear auntie **Nadia**, my second mom, thank you for the care and love you provided me during my five years studies

Also I dedicate this work to our family friend Mister "**Koli Abdellah**" and thank him for the facilities and help that he provided me to achieve my goals

A special dedication goes to someone I am very proud to be related to, my wonderful cousin **Meriem**, you deserve a million thanks and all the hugs that I can give, you are one of the few people in my life who has helped make me into what I am today.

Thank you!

My sincere thanks goes to my beautiful cousins: **Amina, Imane** and **Asma** and to my amazing besties: **Bouchra, Lina** and **Ikrame**, you have been by my side through thick and thin and have always lifted my spirits even when I felt hopeless I'm very blessed to have you in my life

Thank you girls for being my biggest fans!

This dissertation is dedicated to that person who has been always there for me, who kept me moving forward and who made my hard times better.

To "**Abdelouaheb Boudraa**", my best friend



*Amira* 

## Abstract

In this work, Yagi-Uda microstrip patch antennas, conventional and miniaturized, are designed and simulated using the CST software. Initially, the conventional Yagi-Uda with one reflector and two directors is designed after performing a parametric study on the different dimensions of its elements. The resulted structure has shown an improvement in the directivity and radiation pattern as compared to the isolated rectangular patch.

The work is then extended to the design of a miniaturized Yagi antenna. The miniaturization is achieved using a new proposed Defected Microstrip Structure (DMS) that we named '*VASE* defect'. The miniaturized Yagi antenna offers almost the same performances as the conventional with a benefit of a size reduction of about 40%.

To confirm the validity of the designed Yagi antennas, the two antennas are fabricated and their input reflection coefficients are measured and compared with the simulation results. The comparison shows a satisfactory agreement within the measurements conditions.

# Table of Contents

Acknowledgements .....	i
Dedication .....	ii
Abstract .....	iii
Table of contents .....	iv
List of Abbreviations .....	vi
List of Figures .....	vii
List of Tables .....	ix
General Introduction.....	1
<b>Chapter 01: Generalities about Antennas and Defected Microstrip Structure .....</b>	<b>2</b>
1.1 Introduction.....	2
1.2 Fundamental Parameters of Antennas .....	2
1.2.1 Input Impedance .....	2
1.2.2 Reflection Coefficient and VSWR .....	2
1.2.3 Bandwidth .....	3
1.2.4 Radiation Pattern .....	3
1.2.5 Directivity .....	3
1.2.6 Gain .....	4
1.3 Antenna Types .....	4
1.4 Yagi-Uda Antenna .....	4
1.4.1 Definitions and Basic Characteristics .....	4
1.4.2 Operation Principle .....	5
1.5 Overview of Microstrip Patch Antenna .....	6
1.5.1 Definitions and Basic Characteristics .....	6
1.5.2 Principal of Operation of Microstrip Patch Antenna .....	7
1.5.3 Feed Techniques .....	7
1.6 Printed Yagi-Uda Antenna .....	8
1.7 Defected Microstrip Structure .....	9
1.7.1 DMS Overview .....	9
1.7.2 Surface Current Distributions for DMS .....	10
1.7.3 Applications of DMS and Slow-Wave Effect .....	10
1.8 Conclusion .....	11
<b>Chapter 02: Yagi-Uda Microstrip Patch Antenna Design .....</b>	<b>12</b>
2.1 Introduction.....	12
2.2 Design Procedure of Printed Yagi Antenna .....	12
2.3 Structure Geometry Description .....	13
2.4 Effect of Varying the Conventional Planar Yagi Antenna Dimensions .....	14
2.4.1 Effect of the pilot length .....	14
2.4.2 Effect of the Pilot Width .....	14
2.4.3 Effect of the Director Length .....	15
2.4.4 Effect of the Director Width .....	15
2.4.5 Effect of the Reflector Length .....	15
2.4.6 Effect of the Reflector Width .....	16
2.4.7 Effect of the Spacing between the Patch Elements .....	16

2.4.8 Effect of feeding point position $X_p$ .....	17
2.5 Adjustment of the Conventional Planar Yagi Antenna Dimensions .....	17
2.6 Radio-Electric Properties of the Yagi-Uda Antenna .....	19
2.6.1 Input Impedance .....	19
2.6.2 Input Reflection Coefficient .....	19
2.6.3 Bandwidth .....	20
2.6.4 Current Distribution .....	20
2.6.5 Radiation Pattern .....	20
2.7 Conclusion .....	22
<b>Chapter 03: Miniaturization of Yagi-Uda Microstrip Patch Antenna Design .....</b>	<b>23</b>
3.1 Introduction .....	23
3.2 Defect Geometry and Dimensions .....	23
3.3 Simulations Results and Discussion .....	23
3.3.1 Input Impedance .....	23
3.3.2 Input Reflection Coefficient .....	24
3.4 Results of the Reduced Size Printed Yagi-Uda Antenna .....	25
3.4.1 Input Impedance .....	25
3.4.2 Input Reflection Coefficient .....	25
3.4.3 Current Distribution .....	26
3.4.4 Radiation Pattern .....	27
3.4.5 Comparison between the Conventional and Miniaturized Yagi-Uda Antenna .....	28
3.5 Realization and Measurements.....	29
3.5.1 Realization of the Yagi-Uda Antennas .....	30
3.5.2 Measurements of the fabricated Yagi-Uda Antennas .....	30
3.6 Conclusion .....	32
General Conclusion and Further Work .....	33
References .....	x
Appendix .....	xii

## List of Abbreviations

<b>2D</b>	Two-Dimensional
<b>3D</b>	Three-Dimensional
<b>BW</b>	Bandwidth
<b>CST</b>	Computer Simulation Technology
<b>DGS</b>	Defected Ground Structure
<b>DMS</b>	Defected Microstrip Structure
<b>FR-4</b>	Flame Resistant 4
<b>GPS</b>	Global Positioning System
<b>IEEE</b>	Institute of Electrical and Electronics Engineers
<b>RF</b>	Radio Frequency
<b>RFID</b>	Radio Frequency Identification
<b>SWF</b>	Slow Wave Factor
<b>S11</b>	Reflection coefficient
<b>UHF</b>	Ultra High Frequency
<b>VSWR</b>	Voltage Standing Wave Ratio
<b>VHF</b>	Very High Frequency

## List of Figures

<b>Figure 1.1</b> Radiation pattern in spherical coordinates .....	<b>3</b>
<b>Figure 1.2</b> Configuration of a Yagi-Uda antenna .....	<b>5</b>
<b>Figure 1.3</b> Structure of Microstrip patch antenna .....	<b>6</b>
<b>Figure 1.4</b> Electric field lines in microstrip antenna .....	<b>7</b>
<b>Figure 1.5</b> Probe feed of microstrip antenna and its side view .....	<b>7</b>
<b>Figure 1.6</b> Top and side view of 4- elements Microstrip Yagi-Uda Configuration .....	<b>8</b>
<b>Figure 1.7</b> Some DMS Topologies .....	<b>9</b>
<b>Figure 1.8</b> Surface current distributions for rectangular microstrip Patch with slits .....	<b>10</b>
<b>Figure 2.1</b> Yagi microstrip antenna structure geometry .....	<b>13</b>
<b>Figure 2.2</b> The reflection Coefficient of the conventional planar yagi antenna .....	<b>13</b>
<b>Figure 2.3</b> Effect of the pilot length variation on the input reflection coefficient of th4 conventional antenna .....	<b>14</b>
<b>Figure 2.4</b> Effect of the pilot width on the input reflection coefficient of the conventional Yagi antenna .....	<b>14</b>
<b>Figure 2.5</b> Effect of the director length variation on the input reflection coefficient of the conventional Yagi antenna .....	<b>15</b>
<b>Figure 2.6</b> Effect of the director width on the input reflection coefficient of the conventional Yagi Antenna .....	<b>15</b>
<b>Figure 2.7</b> Effect of the reflector length on the input reflection coefficient of the conventional Yagi antenna .....	<b>16</b>
<b>Figure 2.8</b> Effect of the reflector width on the input reflection coefficient of the conventional Yagi antenna .....	<b>16</b>
<b>Figure 2.9</b> Effect of the spacing g on the input reflection coefficient of the conventional Yagi antenna .....	<b>17</b>
<b>Figure 2.10</b> Effect of the feeding point position on the input reflection coefficient of the conventional Yagi antenna .....	<b>17</b>
<b>Figure 2.11</b> Reflection Coefficient of the conventional planar Yagi antenna with the best parametric dimensions .....	<b>18</b>
<b>Figure 2.12</b> The comparison between the Reflection Coefficient of the conventional planar Yagi antenna with different dimensions .....	<b>18</b>
<b>Figure 2.13</b> Input impedance versus frequency of the Yagi Microstrip Antenna with best dimensions .....	<b>19</b>
<b>Figure 2.14</b> Reflection Coefficient of the conventional planar Yagi antenna with the best dimensions .....	<b>19</b>
<b>Figure 2.15</b> Current distribution of the conventional Yagi antenna with the best dimensions at 3 GHz .....	<b>20</b>
<b>Figure 2.16</b> 3D view of the Radiation Pattern at 3 GHz .....	<b>21</b>
<b>Figure 2.17</b> E-plane radiation pattern of the conventional Yagi antenna with the best dimensions at 3 GHz .....	<b>21</b>
<b>Figure 2.18</b> H-plane radiation pattern of the conventional Yagi antenna with the best dimensions at 3 GHz .....	<b>22</b>
<b>Figure 3.1 (a)</b> The Vase Slot Dimensions, <b>(b)</b> Front View of the defected printed Yagi antenna .....	<b>23</b>
<b>Figure 3.2</b> Input impedance versus frequency of the defected printed Yagi-Uda antenna .....	<b>24</b>
<b>Figure 3.3</b> Input reflection coefficient of the defected printed Yagi-Uda antenna .....	<b>24</b>
<b>Figure 3.4</b> Input impedance of the reduced radiating structure .....	<b>25</b>
<b>Figure 3.5</b> Input reflection coefficient of the reduced Yagi-Uda structure .....	<b>26</b>

<b>Figure 3.6</b> (a) The current distribution of the defected printed Yagi antenna (b) The current distribution of the defected Pilot element of the printed Yagi antenna .....	<b>26</b>
<b>Figure 3.7</b> E-plane radiation pattern of the miniaturized Yagi-Uda antenna at 3 GHz .....	<b>27</b>
<b>Figure 3.8</b> H-plane radiation pattern of the miniaturized Yagi-Uda antenna at 3 GHz .....	<b>27</b>
<b>Figure 3.9</b> 3D view of the Radiation Pattern at 3 GHz .....	<b>28</b>
<b>Figure 3.10</b> (a) miniaturized Yagi-Uda antenna, (b) conventional Yagi-Uda antenna .....	<b>29</b>
<b>Figure 3.11</b> Front and back view of both the realized conventional and miniaturized Yagi-Uda patch antennas .....	<b>30</b>
<b>Figure 3.12</b> Vector network analyzer used for $S_{11}$ measurement.....	<b>31</b>
<b>Figure 3.13</b> The input reflection coefficient of the fabricated conventional Yagi antenna .....	<b>31</b>
<b>Figure 3.14</b> The input reflection coefficient of the fabricated miniaturized Yagi antenna .....	<b>31</b>

## List of Tables

<b>Table 2.1</b> Parameters of the dielectric substrate for the yagi antenna .....	<b>12</b>
<b>Table 2.2</b> Dimensions of the initial antenna design .....	<b>12</b>
<b>Table 2.3</b> The best parametric dimensions of the conventional yagi antenna .....	<b>17</b>
<b>Table 2.4</b> New adjusted dimensions of the yagi-uda antenna .....	<b>18</b>
<b>Table 2.5</b> Far field zone Characteristics .....	<b>22</b>
<b>Table 3.1</b> Dimensions of the miniaturized Yagi-Uda antenna .....	<b>25</b>
<b>Table 3.2</b> Far field zone characteristics .....	<b>28</b>
<b>Table 3.3</b> Dimensions of the miniaturized antenna .....	<b>29</b>
<b>Table 3.4</b> Summary of the obtained results .....	<b>29</b>
<b>Table 3.5</b> comparison between the simulated and measured parameters .....	<b>32</b>

# General Introduction

Nowadays, the need of antennas is everywhere due to the innovation in technology in every fields; the antenna is an essential part of a transmitting or receiving system. There exist many forms and types of antennas each of which are characterized by specific features and desirable for a specific use.

To ensure point to point communication within wireless communication systems the requirement for highly directive antenna has been elevated. The main radiation beam of a directive antenna should be towards a particular direction in order to attain a better communication. As well known, Yagi-Uda antennas have high directivity, thus they are popularly used in directive wireless application. Nowadays, microstrip Yagi array, a hybrid of microstrip antenna and Yagi-Uda antenna, have become very popular due to low profile, compatibility with planar component, simple and inexpensive manufacturing process and high directivity. This kind of antenna was first introduced by Huang and Densmore [1].

A typical microstrip Yagi antenna consists of a driven patch element and a few parasitically coupled reflector and Director patch elements [1]. Various attempts have been made to enhance the gain of Yagi antenna by incorporating more than a single director. All these attempts result in an increment in the size of the antenna as well.

Many researchers targeting the size reduction have been conducted and different approaches have been used to achieve this goal such as using high dielectric substrate, shorting post insertion and reshaping antenna by using DGS or DMS techniques. The DMS technique is used in this project because of its simplicity in analysis and realization.

Basically, DMS refers to Defected Microstrip Structure, this technique is based on reshaping the antenna by inserting slots in the radiating patch in order to disturb the current and lengthen its electrical path which results in frequency shift that leads to size reduction.

The aim of this report is to design and analyze a miniaturized microstrip Yagi-Uda antenna using DMS technique and the work is organized in the following three chapters:

**Chapter 1** provides an overview of antenna concepts, covering their various parameters and types, the microstrip patch antenna, the Yagi-Uda antenna, and a combination of two principles that results in a "printed Yagi-Uda antenna" are presented in details. The Defected Microstrip Structure (DMS) technique which is used as a miniaturization technique in order to reduce the overall Yagi-Uda antenna is also explained.

**Chapter 2** investigates the design approach and the analysis of the conventional printed Yagi-Uda antenna where the simulation process is carried out using CST software.

**Chapter 3** demonstrates the technique of miniaturization used where the "Vase" slot is proposed as DMS, and its effect on the printed Yagi antenna is observed. Simulation and results discussion of the proposed antenna with DMS, the comparison between the proposed antenna without DMS and after using DMS technique are all presented. Finally, both the conventional and miniaturized Yagi antennas are fabricated and tested to see how accurate the simulations is

# CHAPTER 1

---

*Generalities about Antennas and Defected  
Microstrip Structure*

# Chapter 01: Generalities about Antennas and Defected Microstrip Structure

## 1.1 Introduction

Wireless technology provides less expensive and a flexible way for communication where antennas are the heart of every wireless communication system. An antenna is defined by Webster's Dictionary as "a usually metallic device (as a rod or wire) for radiating or receiving radio waves." And According to IEEE definitions, an antenna is a mean for radiating or receiving radio waves. In other words the antenna is the transitional structure between free-space and a guiding device [2].

## 1.2 Fundamental Parameters of Antennas

When designing and analyzing an antenna its parameters need to be defined for a good description of its performance. Even though an important number of these parameters exist some of them are selected and they are listed in the following section.

### 1.2.1 Input Impedance

It is defined as "the impedance presented by an antenna at its terminals or the ratio of the voltage to the current at the pair of terminals or the ratio of the appropriate components of the electric to magnetic fields at a point. Hence the impedance of the antenna can be written as

$$Z_{in} = R_{in} + jX_{in} \quad (1-1)$$

Where:

- $Z_{in}$  is the antenna impedance
- $R_{in}$  is the antenna resistance
- $X_{in}$  is the antenna reactance.

The imaginary part  $X_{in}$  of the input impedance represents the power stored in the near field of the antenna while the resistive part,  $R_{in}$ , consists of two components the radiation resistance  $R_r$  and the loss resistance  $R_L$ . The power associated with the radiation resistance is the power actually radiated by the antenna, while the power dissipated in the loss resistance is lost as heat in the antenna itself due to dielectric or conducting losses [3].

### 1.2.2 Reflection Coefficient and VSWR

For an antenna to perform efficiently there is always a reflection of the power, which leads to the standing waves. The amount of reflected power is quantified using the reflection coefficient or ( $S_{11}$  the S parameter at the antenna input) [4], defined as:

$$\Gamma = \frac{Z_{in} - Z_0}{Z_{in} + Z_0} \quad (1-2)$$

Where:

- $Z_{in}$  is the antenna input impedance
- $Z_0$  is the feeding line/probe characteristic impedance

Another parameter providing almost the same information as the reflection coefficient is the VSWR. The VSWR is defined as the ratio of the maximum RF voltage  $V_{max}$  to the minimum  $V_{min}$  along the transmission line and it is given by:

$$VSWR = \frac{V_{max}}{V_{min}} = \frac{1+|\Gamma|}{1-|\Gamma|} \quad (1-3)$$

The minimum possible value of VSWR is unity and this corresponds to a perfect match [4].

### 1.2.3 Bandwidth

The bandwidth of an antenna is defined as the range of frequencies within which the performance of the antenna, with respect to some characteristic, conforms to a specified standard, In other words it is the range of frequencies, on either side of a center frequency where the antenna characteristics are within an acceptable value of those at the center frequency. [2]This bandwidth, BW, is defined as:

$$BW = \frac{f_2 - f_1}{f_0} \times 100\% \quad (1-4)$$

Where:

- $f_1$  and  $f_2$  are the lower and upper cut of frequencies of the band respectively. In antennas these limits correspond to frequencies for which their reflection coefficient reaches – 10 dB
- $f_0$  is the centre frequency of the operating band.

### 1.2.4 Radiation Pattern

The radiation pattern is defined as a mathematical function or a graphical representation of the radiation properties of the antenna (Power flux density, radiation intensity, and directivity) as a function of space coordinates. It provides information which describes how an antenna directs the energy it radiates [4]. In other words it is a plot of the far-field radiation properties of as a function of the spatial coordinates which are specified by the elevation angle ( $\theta$ ) and the azimuth angle ( $\phi$ ).It can be plotted as a 3D graph or as a 2D polar or Cartesian slice of this 3D graph [3]. Typically, the elevation plane contains the electric-field vector (E-plane) and the direction of maximum radiation, and the azimuth plane contains the magnetic-field vector (H-Plane) and the direction of maximum radiation as illustrated in Figure1.1 [4].

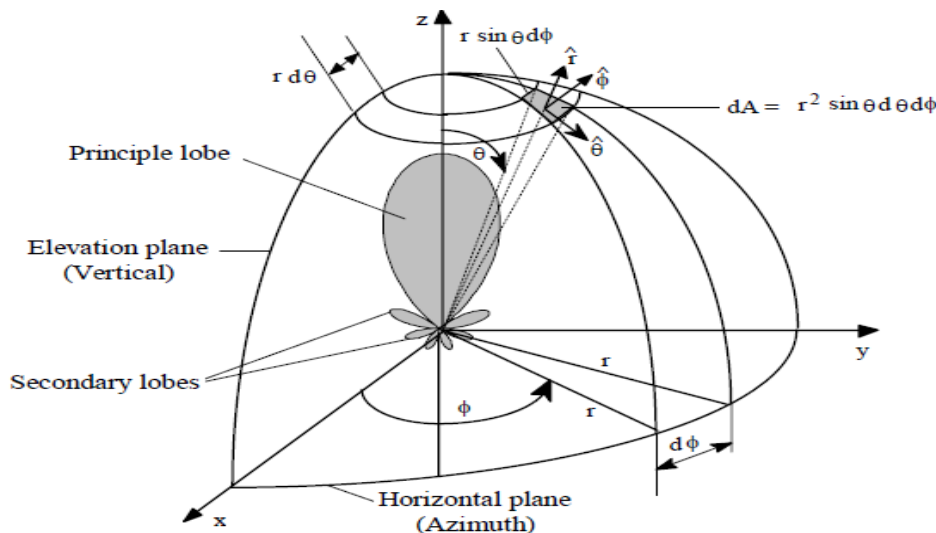


Figure 1.1 Radiation pattern in spherical coordinates [4]

### 1.2.5 Directivity

Directivity of an antenna is defined as the ratio of the radiation intensity in a given direction from the antenna to the radiation intensity averaged over all directions. The average radiation intensity is equal to the total power radiated by the antenna divided by  $4\pi$ . Stated more simply; the directivity of a non-isotropic source is equal to the ratio of its radiation intensity in a given direction over that of an isotropic source [2] and it is given by:

$$D(\theta, \varphi) = \frac{4\pi U(\theta, \varphi)}{P_{\text{rad}}} \quad (1-5)$$

Where:

- $U$  is the radiation intensity in (W/unit solid angle).
- $P_{\text{rad}}$  is total radiated power in (W).

### 1.2.6 Gain

Gain of an antenna is defined as the ratio of the intensity in a given direction, to the radiation intensity that would be obtained if the power accepted by the antenna were radiated isotropically. The radiation intensity corresponding to the isotropically radiated power is equal to the power accepted (input) by the antenna divided by  $4\pi$ . It's expressed as [2]:

$$\text{Gain} = G = \frac{4\pi U}{P_{\text{in}}} \quad (1-6)$$

Where:  $G$  is the Gain and  $U$  is the radiation intensity and  $P_{\text{in}}$  is the total input power. Also it is defined as antenna directivity times a factor representing the total efficiency. It is given by

$$G = D \times e_T \quad (1-7)$$

Where:

- $D$  is the directivity of the antenna
- $e_T$  is the total efficiency of the patch antenna that is given by:

$$e_T = e_r(1 - |\Gamma|) \quad (1-8)$$

- $e_r$  is the radiation efficiency given by

$$e_r = \frac{P_{\text{rad}}}{P_{\text{in}}} = \frac{R_r}{R_{\text{in}}} \quad (1-9)$$

## 1.3 Antenna Types

Since the start of radio communications over 100 years ago, thousands types of antennas have been developed varying in shapes, characteristics, aspects and applications, the most familiar are wire antennas because they are seen everywhere, on automobiles, aircraft and ships, they are made out of conductors and can take several forms like a dipole, loop, helix and Yagi-Uda. Other familiar antennas are the apertures, which are used in the microwave applications. Also there exist parabolic reflectors, aggregate arrays and microstrip patch antennas. The last type is widely used because of its several advantages over conventional microwave antennas [4].

### 1.4 Yagi–Uda Antenna

The Yagi–Uda antenna is a popular type of end fire antenna widely used in the VHF and UHF bands because of its simplicity, low cost and relatively high gain [5]. During the early days of its discovery the antenna was mainly used in Televisions but later, such antennas found applications in all other fields like Radars, RFID's, Satellites[6]. Yagi and Uda were two Japanese professors who invented and studied this antenna in the 1920s. Uda made the first Yagi–Uda antenna and published the results in Japanese in 1926, and the design was further developed and published in English by his colleague Professor Yagi a year later [5].

#### 1.4.1 Definitions and Basic Characteristics

The Yagi antenna is a highly directional antenna in the sense that it radiates greater power in one direction thereby reducing the interference from all other sources [6]. The main feature of this directional antenna is that it consists of two kinds of elements one is the driven element

which is the main radiating element and the other is parasitic elements added which are not directly connected to the driven element, the ones in the forward beam act as directors while the one in the rear act as reflectors. These different elements are described as follow and illustrated in Figure 1.2

**The driven element:** It's the heart of the antenna where the feeding is usually provided towards the center of the dipole so that maximum power transfer takes place from transmitters to antennas [6]. A dipole is said to be resonant when its length is slightly less than  $\lambda/2$ , usually  $(0.45-0.49)\lambda$ [2]. The dipoles need not be always linear in structure, it may be folded also [6].

**The reflector:** It is usually placed at the end of the driven element. The length of a reflector is slightly longer than that of a driven element but its frequency of operation is less than the driven element [6], its role is to force the radiated energy towards the front. It exhibits an inductive reactance. The length of the reflector and the spacing has a large effect on the front-to-back ratio and antenna input impedance where the optimum spacing between the reflector and the driven element is between  $(0.15-0.25)\lambda$  [5].

**The director:** It is a highly resonant structure and operates at a frequency higher than the driven element [6]; usually 10 to 20% shorter than the resonant driven element and appear to direct the radiation towards the front. They are of capacitive reactance. The director to driven element spacing is typically 0.25 to 0.35 wavelengths. [5]. the number of directors used may depend on the physical size of the antenna and increasing the number of directors may enhance the maximum achievable directivity and gain of the antenna. The length and spacing of a director has significant effect on the forward and backward gain and provides the antenna with a directional radiation pattern [6].

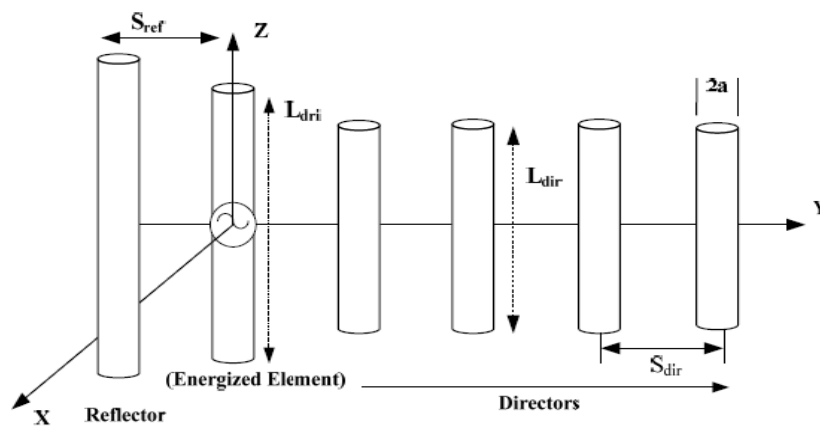


**Figure 1.2** Configuration of a Yagi-Uda antenna [7]

Each of these dipole elements are arranged on a supporting boom structure. The reflector and the director are designed to be in parasitic mode, since no feeding is provided to these elements. The position of first director element and the spacing of reflectors decides the matching of the Yagi antenna and its gain depends on the number of array elements. As the number of elements increases, the gain increases provided the elements are not separated far apart and they are equal in length [7].

### 1.4.2 Operational Principle.

The radiation towards the back seems to be blocked by the longer element; the reflector and director produce push-and-pull effects on the radiation [5]. The parasitic elements of the Yagi antenna operate by picking up power from the dipole re-radiating their signals in a slightly

different phase to that of the driven element. The phase is in such a manner affects the properties of the RF antenna as a whole, causing power to be focused in one particular direction and removed from others. In this way the signal is reinforced in some directions and cancelled out in others [7].

The field provided by the driven element induces currents in the parasitic elements of the array through mutual coupling [6]. These induced currents form a traveling wave structure at the desired frequency. The performance is determined by the current distribution in each element and the phase velocity of the traveling wave. The current distribution on the driven element is determined by its length, frequency and coupling with nearby elements (mainly the reflector and first director). The dominant current is on the driven element, the reflector and the first director carry less current, and the currents on other directors are further reduced and they appear to be of similar amplitude, which is typically less than 40% of that of the driven element [5].

The yagi antenna exhibits a directional pattern consisting of a main forward lobe and a number of spurious side lobes [7]. One of the figures associated with the Yagi antenna gain is what is termed the front to back ratio. This is simply a ratio of the signal level in the forward direction to the reverse direction. It is normally expressed in dB [8].

$$\text{Front to back ratio} = \frac{\text{Signal in forward direction}}{\text{Signal in reverse direction}} \quad (1-10)$$

## 1.5 Overview of Microstrip Patch Antenna

Microstrip antennas are among the most widely used types of antennas, they have several advantages over conventional microwave antenna. Because of their simplicity and with printed-circuit technology, making them easy to manufacture either as stand-alone elements or as elements of arrays. The advantages microstrip antennas make them suitable for various applications like vehicle-based satellite link antennas and global positioning systems (GPS).

### 1.5.1 Definitions and Basic Characteristics

Microstrip patch antenna consists of a radiating patch on one side of a dielectric substrate which has a ground plane on the other side as shown in Figure 1.3. The patch is generally made of conducting material such as copper or gold and can take any possible shape, it is generally square, rectangular, circular, triangular, elliptical or some other common shape. For a rectangular patch, the length  $L$  of the patch is usually  $0.3333\lambda_0 < L < 0.5\lambda_0$ , where  $\lambda_0$  is the free-space wavelength. The patch is selected to be very thin such that  $t \ll \lambda_0$  (where  $t$  is the patch thickness). The height  $h$  of the dielectric substrate is usually  $\lambda_0/3 \leq h \leq \lambda_0/2$ . The dielectric constant of the substrate is typically in the range  $2.2 \leq \epsilon_r \leq 12$  [2].

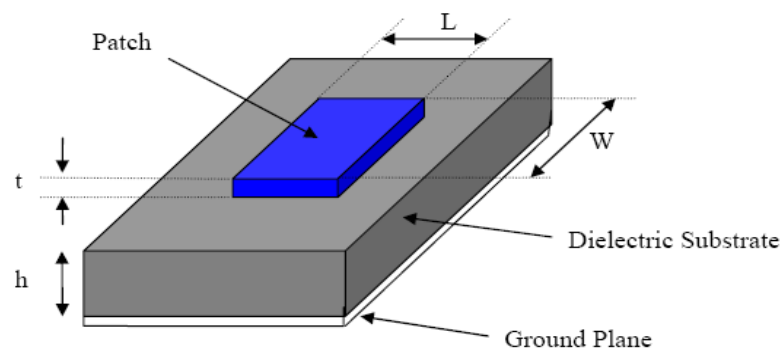


**Figure 1.3** Structure of Microstrip patch antenna [9]

### 1.5.2 Principle of Operation of Microstrip Patch Antenna

Microstrip antenna is a transducer which transmits or receives electromagnetic waves. Figure 1.4 shows the field lines in a non-homogenous medium composed generally by air and substrate. Typically most of the field lines lie in the substrate and parts exit in air. Since part of the waves travel in the substrate and part in air, an effective dielectric constant  $\epsilon_{eff}$  is introduced to account for fringing and wave propagation in the line. Therefore, the performances of the microstrip patch sensor will be affected by effective dielectric constant  $\epsilon_{eff}$  of the substrate and the dimension of patch [9].

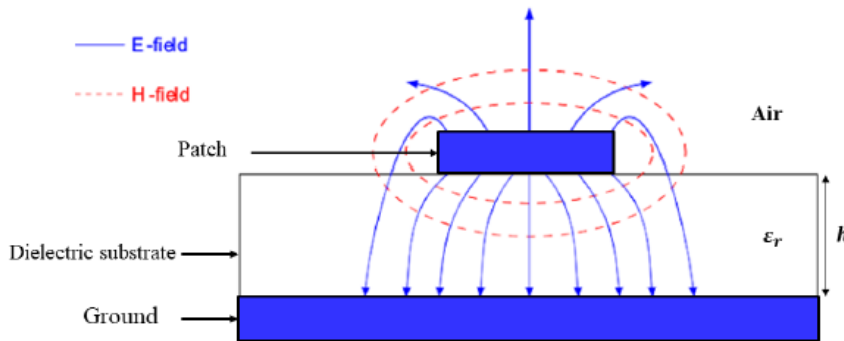


Figure 1.4 Electric field lines in microstrip antenna [9]

Fringing effect comes due to electric field lines which makes the antenna size wider after excitation. The main cause of fringing effect is due to width and position of feed in antenna, and it's the responsible of the radiation mechanism and give more directive radiation pattern but resonant frequency is shifted from the desired frequency [9].

### 1.5.3 Feed Techniques

Microstrip patch antennas can be fed by a variety of methods. These methods can be classified into two categories- contacting and non-contacting. In **the contacting method**, the RF power is fed directly to the radiating patch using a connecting element such as a microstrip line. In the **non-contacting scheme**, electromagnetic field coupling is done to transfer power between the microstrip line and the patch. The four most popular feed techniques used are the microstrip line, coaxial probe, aperture coupling, and proximity coupling [10].

The method that's going to be used in this project is Coaxial-Line Feed where patch is fed along center line; the inner conductor of the coaxial connector extends through the dielectric and is soldered to the radiating patch, while the outer conductor is connected to the ground plane as shown in Figure 1.5. The main advantages of this arrangement are that the feed can be placed at any desired location inside the patch to match it with its input impedance [10].

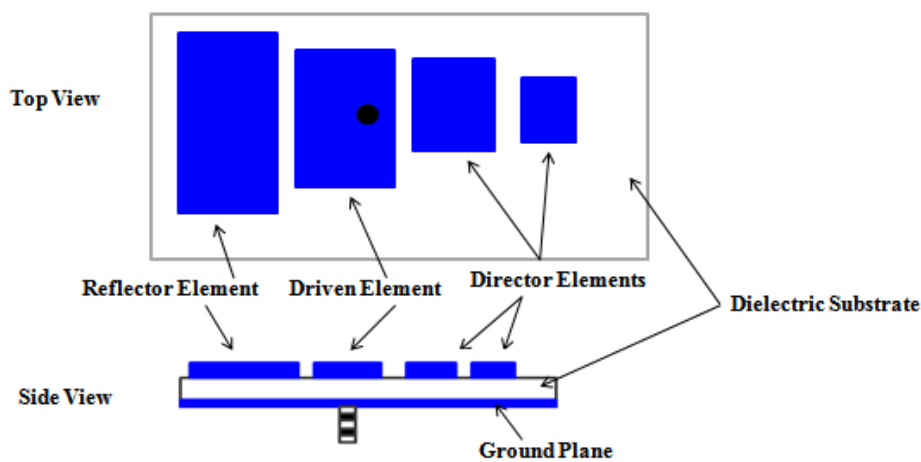


Figure 1.5 Probe feed of microstrip antenna and its side view [9]

## 1.6 Printed Yagi-Uda Antenna

Printed Yagi-Uda antenna is an antenna structure that combines Yagi-Uda array and microstrip patch antenna concepts where the first printed Yagi-Uda antenna design was suggested by Huang in 1989.

The microstrip Yagi antenna, as illustrated in Figure 1.6 consists of a driven patch element and a few parasitically coupled reflector and director patch elements. It utilizes a similar principle as a conventional Yagi-Uda dipole array where the electromagnetic energy is coupled from the driven element dipole through space into the parasitic dipoles and then reradiated to form a directional beam. However in a microstrip Yagi array, the electromagnetic energy is coupled from the driven patch to the parasitic patches not only through space but also by surface waves in the substrate [11].



**Figure 1.6** Top and side view of 4- elements Microstrip Yagi-Uda Configuration

In array applications, mutual coupling effect is often considered undesirable, since it reduces the antenna gain and raises the side lobe level. However, in some applications mutual coupling enhances the antenna performance. For example, in the case of microstrip antenna, parasitic patches can be placed around a driven element to increase the gain of this single driven element by several decibels. It was empirically determined that the dimension ratio of the reflector patch to the driven element patch is somewhere between 1.1 to 1.3, depending on the substrate thickness and dielectric constant and The dimension ratio between the director patch and the driven element patch should be between 0.8 and 0.95 [12].

In conventional Yagi-Uda antenna the dipole radiates RF power equally around its axis; it can couple relatively strong power to its neighbors, even when the spacing between dipoles is large. The microstrip patch, on the other hand, radiates primarily in its broadside direction, and very little along the direction of the ground plane. This is why a microstrip patch generally couples very little energy to its neighboring patches, especially when the patches' separation becomes large. As a consequence, in order for the microstrip patches to function similarly to the Yagi dipoles, the adjacent patches need to be placed very closely to each other so that a significant amount of coupling can be obtained through surface waves in the

substrate .It was found experimentally that the gap distance between two patch edges should be equal to or less than the dielectric substrate thickness [11].

### 1.7 Defected Microstrip Structure

In all areas of electrical engineering, especially in electronic devices and computers, the attention has been shifted toward miniaturization. Particularly in antennas; a large emphasis in the last few years has been placed toward electrically small antennas, including printed circuits board designs. For very low frequencies of MHz range, the size of the microstrip antennas becomes too large to be manageable hence miniaturization is needed to reduce the overall space occupied in the communication system.

Various techniques were introduced in order to fulfill this purpose such as:

- Varying dielectric material properties of the substrate.
- Shorting post insertion.
- Reshaping antenna by introducing slots in ground plane which is known as DGS or in the patch which is known as DMS or a combination of them [13].

In this section, we will discuss miniaturization based on defected microstrip structure. The choice of this technique is simply motivated by its simplicity in analysis and realization.

#### 1.7.1 Defected Microstrip Structure Overview

In the past, the defected ground structure has been widely employed for RF circuit design and improving RF components performance. A DGS unit is made by etching patterns in the ground plane of a microstrip line and it increases its effective capacitance and inductance. However, DGS introduces wave leakage through the ground plane hence defects on the ground plane causes more severe degradation in the transmission line performance; to overcome this problem the DMS is used instead [14].The DMS refers to a defect inserted in the microstrip line. It is made by etching shaped slots in the microstrip structure hence no leakage through the ground plane can take place [15] Figure1.7 shows some different shape and size of slotted microstrip antennas.

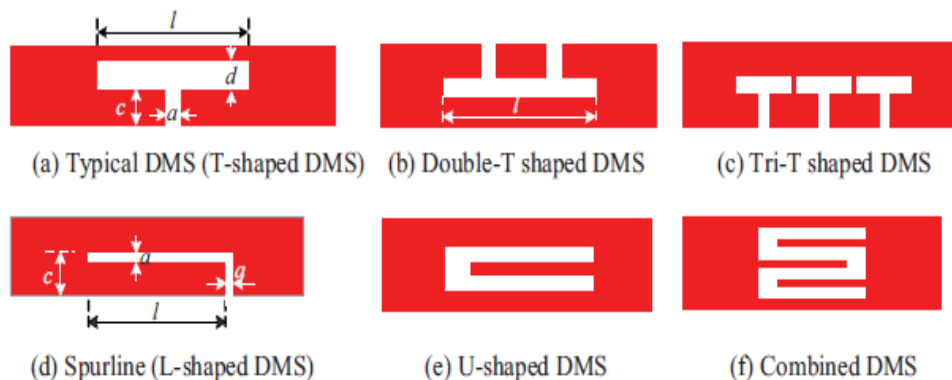


Figure1.7 Some DMS topologies [14]

By etching slots in the antenna radiating patch, the surface current is disturbed and the electrical length of the microstrip antenna gets lengthened. Consequently, the resonance frequency is significantly decreased. This shift of frequency leads to size miniaturization [15].

DMS has a higher effective inductance compared with DGS. It has been proved that the effective inductance in DMS is much larger than that in DGS with the same etched area, but they nearly have the same values of capacitance, Moreover DMS is more easily integrated with other microwave circuits, and it has an effectively reduced circuit size compared with DGS [13].

### 1.7.2 Surface Current Distributions for DMS

Meandering the excited patch surface current paths in the antenna's radiating patch is an effective method for achieving size reduction of the microstrip antenna. For the case of a rectangular radiating patch. The meandering can be achieved by inserting several narrow slits at the patch's non radiating edges. It can be seen in Figure 1.8 that the excited patch's surface currents are effectively meandered, leading to a greatly lengthened current path for a fixed patch linear dimension. This behavior results in a greatly lowered antenna fundamental resonant frequency, and thus a large antenna size reduction at a fixed operating frequency can be obtained [16].

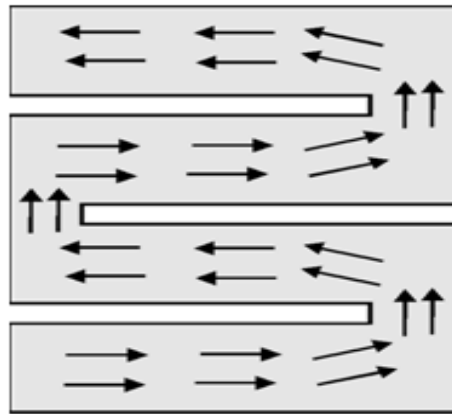


**Figure 1.8** Surface current distributions for rectangular microstrip Patch with slits [16]

### 1.7.3 Applications of DMS and Slow-Wave Effect

A DMS structure is of great advantage for designing RF components because of a reduction of size and electromagnetic interference noise immunity. Moreover, DMS exhibits the properties of slow-wave, rejecting microwaves in certain frequencies, which are similar to the well-known DGS but without any manipulation of the ground plane [14].

DMS presents a greater slow wave effect, since it has more discontinuities, providing a longer trajectory to the electromagnetic wave. The use of DMS allows an increase in slow wave factor in transmission lines in which they are introduced. This phenomenon can be used to reduce the size of passive planar circuits like microstrip line lengths, coupling lines and microstrip antennas, among other microstrip structures [17].

The **SWF** is the relationship between the wave number in free space,  $\mathbf{K}_0$ , and the propagation constant,  $\beta$ , of the transmission line

For lossless microstrip line, the SWF is determined by:

$$SWF = \frac{\beta}{K_0} = \sqrt{\epsilon_{reff}} = \frac{\lambda_0}{\lambda_g} \quad (1.11)$$

With  $\lambda_0$  and  $\lambda_g$  are respectively the free space and the propagation wave length and the propagation constant is determined by:

$$\beta = \sqrt{\epsilon_{\text{reff}}} K_0 \quad (1.12)$$

Where  $\epsilon_{\text{reff}}$  is the effective permittivity of the material.

The SWF of a microstrip line is raised when a discontinuity is introduced in the path of the electromagnetic wave, increasing the impedance of the line [17]. In addition to slow wave effect DMS are mostly used to enhance the performances of various planar passive circuits and to filter certain spurious signals, and also used as a tuning technique for rectangular patch antennas.

## 1.8 Conclusion

In this chapter generalities about the antenna and its different parameters and types was introduced. An overview of wire Yagi-Uda antenna and microstrip antenna were presented as well as the Printed Yagi-Uda antenna. Finally one of the miniaturization techniques called DMS was explained.

# CHAPTER 2

---

*Design and Analysis of Yagi-Uda Microstrip  
Patch Antenna*

## Chapter 02: Design and Analysis of Yagi-Uda Microstrip Patch Antenna

### 2.1 Introduction

In this chapter, Yagi-Uda microstrip patch antenna is designed to operate at 3 GHz which is the RADAR frequency. The antenna is excited with a coaxial probe and the simulation process is done by the CST simulator software. The design is carried out based on theory that has been outlined in chapter one. A parametric study is done on the dimensions of the proposed structure to enhance its performance

### 2.2 Design Procedure of Printed Yagi Antenna

The first step of the design procedure is started by designing a single element which a Rectangular patch called a driven element. According to the empirical models reported in literature the patch dimensions are given by:

The Width:

$$W = \frac{1}{2f_r \sqrt{\mu_0 \epsilon_0}} \sqrt{\frac{2}{\epsilon_r + 1}} = \frac{c}{2f_r} \sqrt{\frac{2}{\epsilon_r + 1}} \quad (2-1)$$

The effective permittivity used in the patch length calculation is:

$$\epsilon_{reff} = \left(\frac{\epsilon_r + 1}{2}\right) + \left(\frac{\epsilon_r - 1}{2}\right) \frac{1}{\sqrt{1 + 12 \frac{h}{W}}} \quad (2-2)$$

Extension due to the fringing effect used in the patch length calculation is:

$$\Delta L = 0.412h \times \frac{(\epsilon_{reff} + 0.3) \left(\frac{W}{h}\right)^{0.264}}{(\epsilon_{reff} - 0.258) \left(\frac{W}{h}\right)^{0.8}} \quad (2-3)$$

Finally, the length is given as:

$$L = L_{eff} - 2\Delta L = \frac{c}{2f_r \sqrt{\epsilon_{reff}}} - 2\Delta L \quad (2-4)$$

Using the equations (2.1) through (2.4) we obtain: **W = 30.71 mm** and **L = 23.70 mm**.

The second step of the design procedure is accomplished by adding parasitic patch elements; the ones in the forward beam act as directors while the one in the rear acts as a reflector. This antenna has been designed using the FR4 lossy dielectric substrate which has the parameters given in table 2.1:

**Table 2.1** Parameters of the dielectric substrate for the Yagi antenna

The operating frequency $f_r$	The dielectric constant $\epsilon_r$	loss tangent tang $\delta$	The dielectric height h
3 GHz.	4.3	0.017	1.63 mm

The theoretical dimensions of the printed Yagi antenna are calculated using the principle given in section 1.6 and the obtained values are summarized in table 2.2.

**Table 2.2** Dimensions of the initial antenna design

Elements	Length (mm)	Width (mm)
Reflector	26.07	33.78
Driven Patch	23.70	30.71
Director	18.96	24.68

### 2.3 Structure Geometry Description

The shape of a conventional 4 elements planar Yagi antenna is shown in figure 2.1

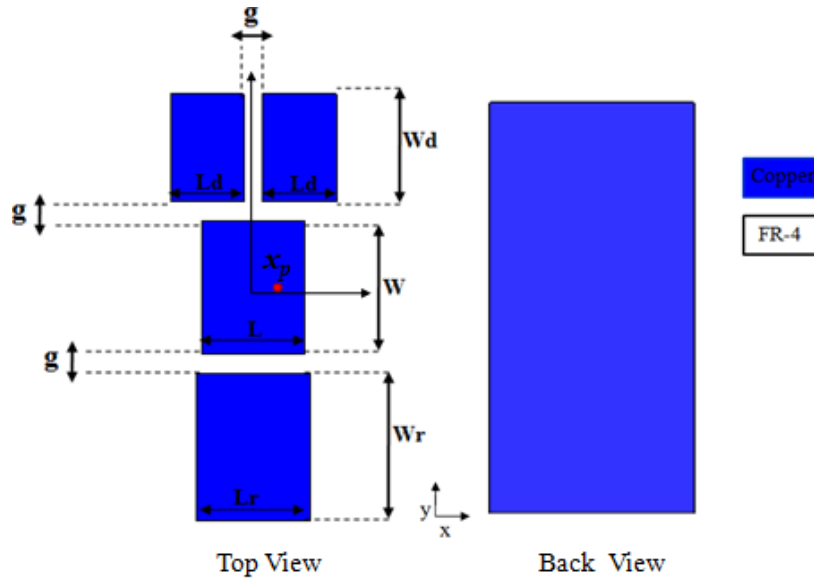


Figure 2.1 Yagi Microstrip antenna structure geometry

The conventional 4-elements planar Yagi antenna consist of a reflector R and Pilot P and two directors  $D_1$  and  $D_2$  that are used to establish the directionality of the beam as well as to increase the antenna gain by several decibels

In order to make more power coupled to the directors from the driven element and increase the field strength, the two directors are added in parallel and symmetrically above the driven patch. Moreover, two director patches and one reflector patch are enough because the increasing number of the parasitic patches cannot improve the antenna characteristics, but enlarge the geometric size of the antenna. The distance between these elements along the axis is denoted by  $g = 4.3 \text{ mm}$ .

The proposed structure with dimensions given in table 2.2 along with substrate dimensions of  $130 \times 60 \text{ mm}$  and  $x_p = 5.5 \text{ mm}$ , chosen arbitrary, is simulated using CST software. The obtained reflection coefficient  $|S_{11}|$  of the antenna is illustrated in figure 2.2.

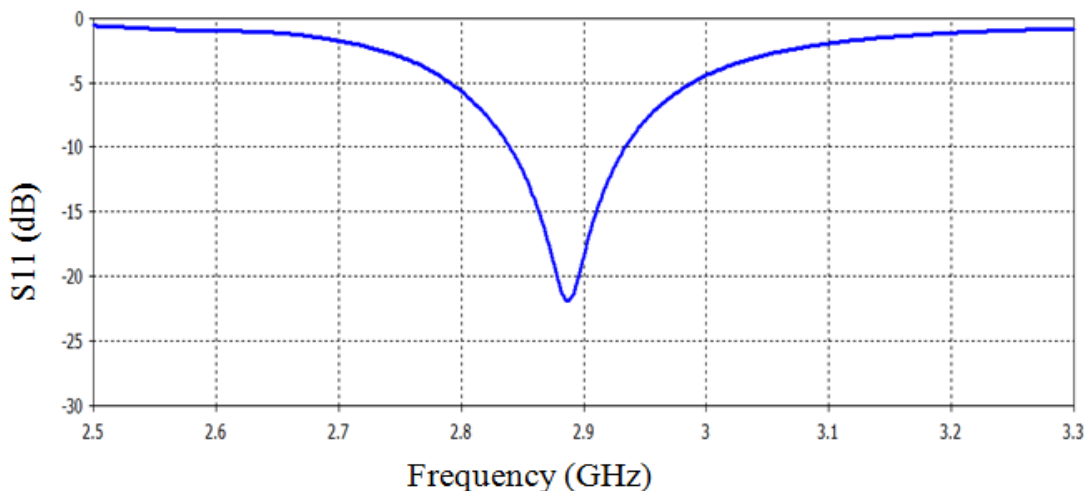


Figure 2.2 the reflection Coefficient of the conventional planar Yagi antenna

It can be noticed from figure 2.2 that the antenna is matched at the frequency of 2.88 GHz because the reflection coefficient value is less than -10 dB but it is not at the desired frequency thus a readjustment of the dimensions is required to get good matching at the frequency of 3 GHz.

## 2.4 Effect of Varying the Conventional Planar Yagi Antenna Dimensions

The parametric study of the proposed antenna dimensions is done to visualize the effect of these different parameters on the antenna performance

### 2.4.1 Effect of the Pilot Length

By varying the length around the theoretical value obtained previously, the obtained simulated reflection coefficient is illustrated in figure 2.3. As expected, the increase in the pilot length results in the decrease in the resonant frequency. Also, the figure indicates that the convenient value of pilot length for the 3 GHz is  $L = 22.644$  mm.

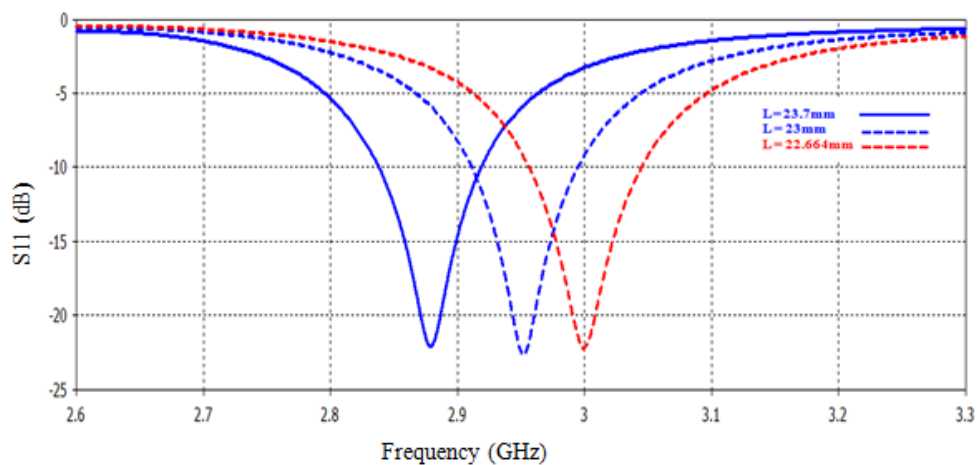


**Figure 2.3** Effect of the pilot length variation on the input reflection coefficient of the Yagi-Uda antenna

### 4.2.2 Effect of the Pilot Width

In a similar manner to the length, the width is also varied around the empirical value obtained previously and the effect of this variation is illustrated in figure 2.4. This parameter does not affect highly the resonant frequency instead it influences the matching. By decreasing the width, the matching becomes better as the case of  $W = 28.71$  mm.

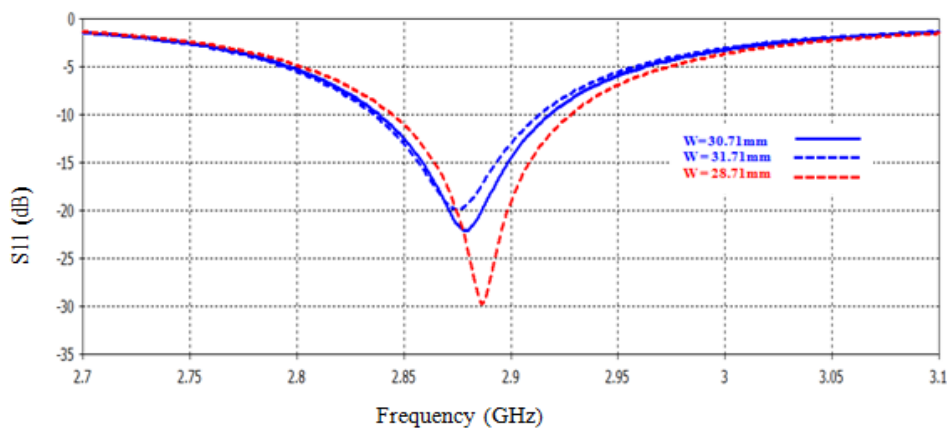


**Figure 2.4** Effect of the pilot width on the input reflection coefficient of the conventional Yagi antenna

### 2.4.3 Effect of the Director Length

As in the previous study, the director length is varied around its empirical value; the effect of this variation is shown in figure 2.5 (zoomed around the lower values of  $S_{11}$ ). This variation does not have an important effect on the input reflection coefficient of the antenna.

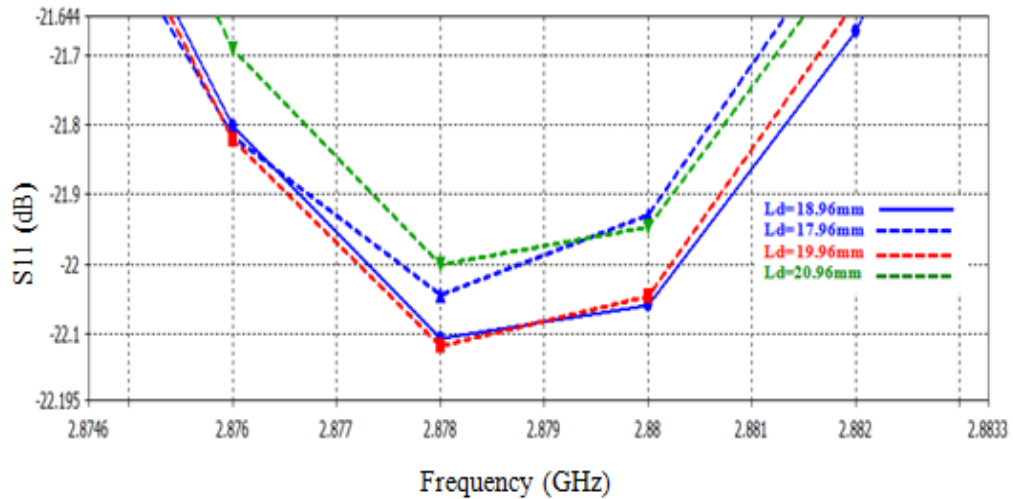


**Figure 2.5** Effect of the director length variation on the input reflection coefficient of the conventional antenna

### 2.4.4 Effect of the Director Width

Figure 2.6 shows the simulated reflection coefficient produced by altering the director width around the theoretical value acquired before. The figure shows insignificant variation of  $S_{11}$  when varying the director width.

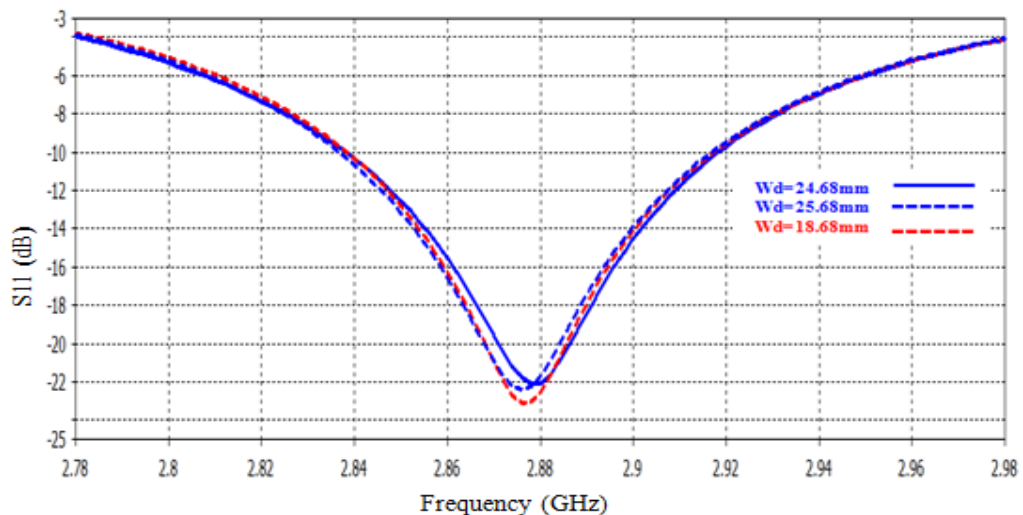


**Figure 2.6** Effect of the director width on the input reflection coefficient of the conventional Yagi Antenna

### 2.4.5 Effect of the Reflector Length

Likewise the reflector length is varied about the theoretical value obtained before in the same way as in the previous cases. An increase in the reflector length results very small decrease in the resonant frequency and level of  $S_{11}$  as shown in figure 2.7.

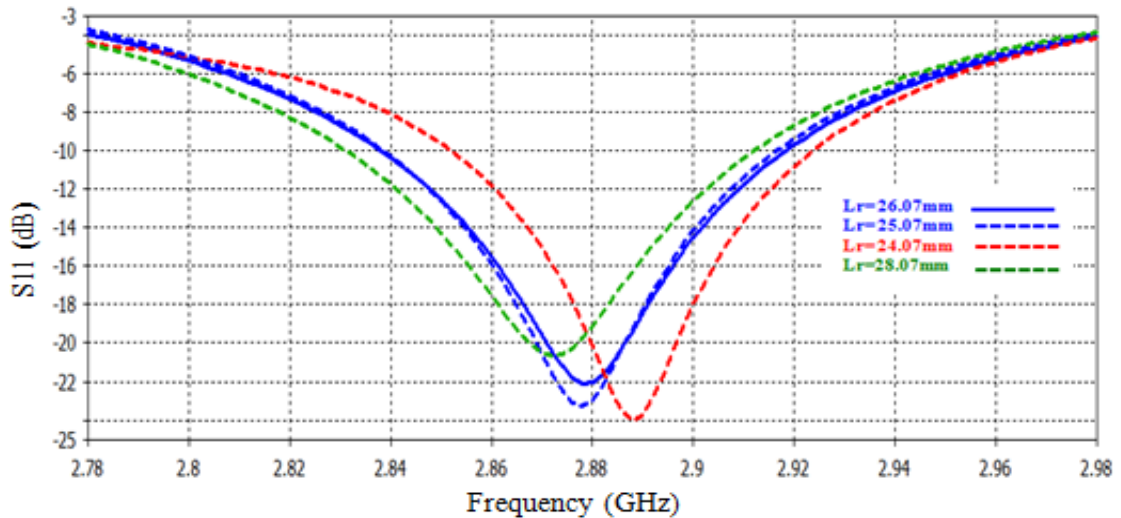


**Figure 2.7** Effect of the reflector length on the input reflection coefficient of the conventional Yagi antenna

#### 2.4.6 Effect of the Reflector Width

Figure 2.8 illustrates the simulated reflection coefficient obtained by varying the reflector width around its theoretical value. It is clearly seen that the width of the reflector affects insignificantly the input reflection coefficient of the Yagi-Uda antenna.

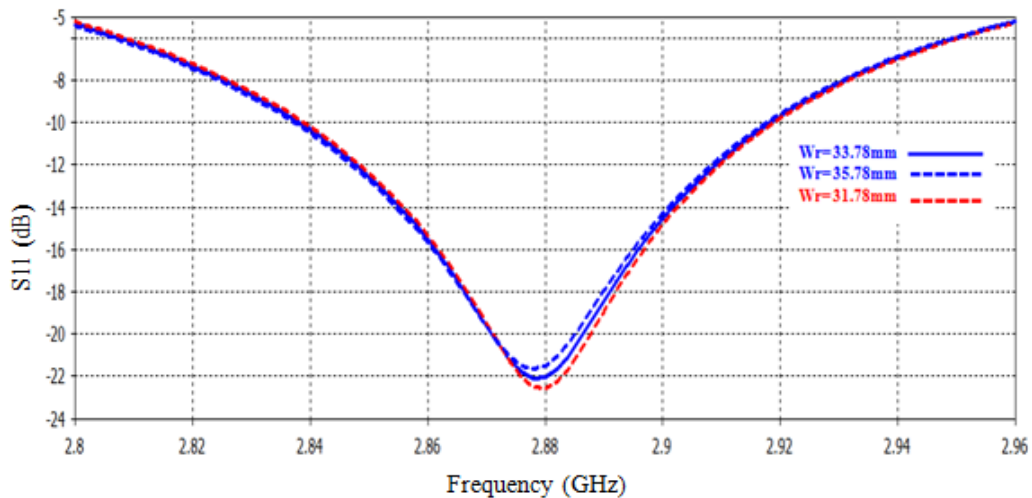


**Figure 2.8** Effect of the reflector width on the input reflection coefficient of the conventional Yagi Antenna

#### 2.4.7 Effect of the Spacing between the Patch Elements

The input reflection coefficient is shown in figure 2.9. By varying the distance between the patch elements in Yagi antenna around the theoretical value 4.3mm, it is clearly noticeable that a decrease in the spacing,  $g$ , results in a small increase in the resonant frequency with a diminution in the level of return loss.

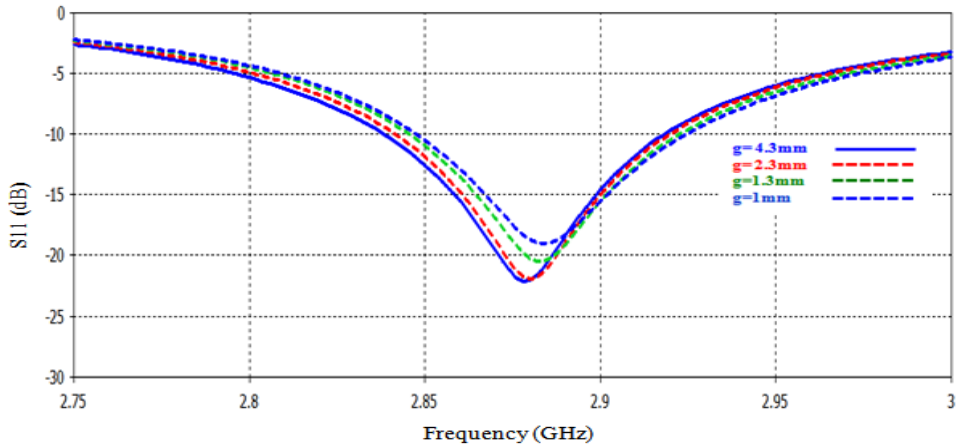


**Figure 2.9** Effect of the spacing  $g$  on the input reflection coefficient of the conventional Yagi antenna

### 2.4.8 Effect of Feeding Point Position $X_p$

In the proposed design, a discrete port is used to feed the antenna, which is in CST equivalent to 50 Ohm. The feed port is varied at different coordinates across the  $x$ -axis from the patch center to its edge as shown in figure 2.10. It is evident that as we approach the point to a coordinate of  $x_p = 6.5$  mm from the center of the patch good matching would be realized, that is the input impedance of the antenna comes toward 50 ohm.

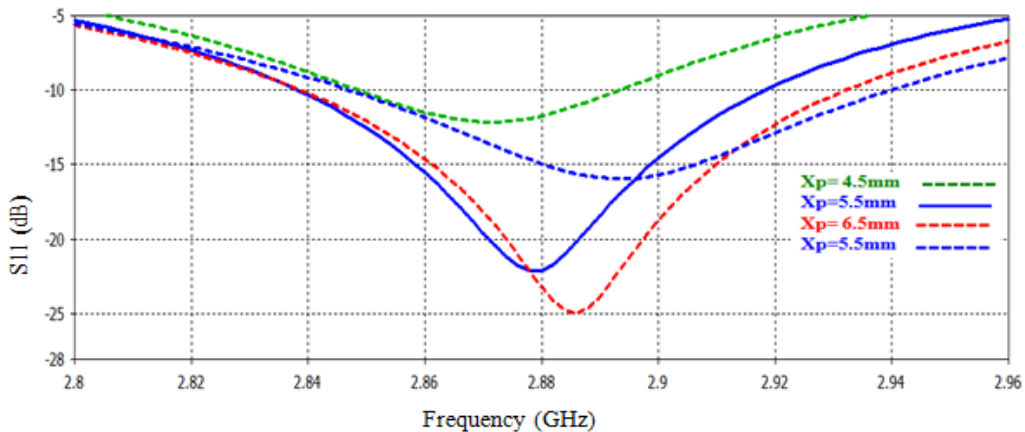


**Figure 2.10** Effect of the feeding point position on the input reflection coefficient of the conventional Yagi antenna

## 2.5 Adjustment of the Dimensions of the Conventional Planar Yagi-Uda Antenna

To have acceptable radio-electric properties of the conventional Yagi-Uda antenna, the best values of the structure parameters from the previous studies are chose as summarized in table 2.3. The input reflection coefficient of the antenna with these values is drawn as illustrated in figure 2.11.

**Table 2.3** The best parametric dimensions of the conventional Yagi-Uda antenna

Elements	Length (mm)	Width (mm)
Le Reflector	24.07	31.78
Driven Patch	22.664	28.71
Director	19.96	18.68

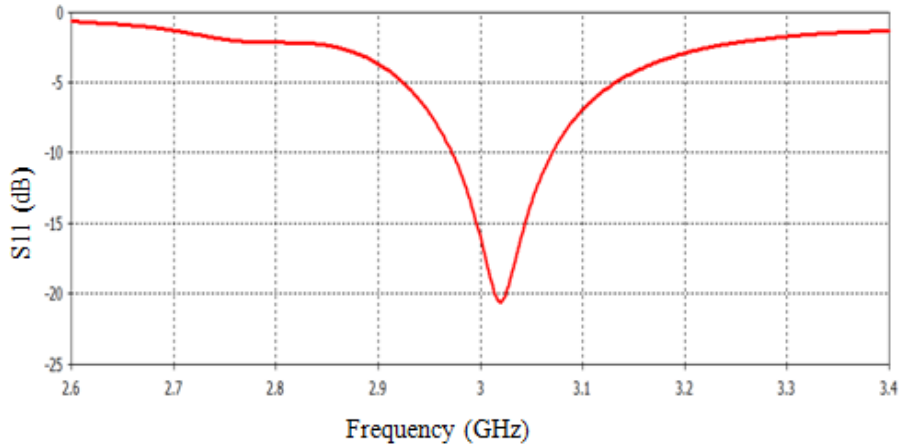


**Figure 2.11** Reflection Coefficient of the conventional planar Yagi antenna with the best parametric dimensions

Due to the high dependency of the Yagi-Uda antenna performances to its parameters, the tuning to the 3GHz frequency and a good impedance matching required small adjustment in all dimensions. This is performed by several simulations attempts and the resulted dimensions that produce the exact resonance frequency, 3 GHz and a satisfactory matching between the input impedance and the probe characteristics impedance are summarized in the table 2.4. The used feed point position is **(6.7 mm, 0)** and spacing **g** of **2.5 mm**.

**Table 2.4** New adjusted dimensions of the Yagi-Uda antenna

Elements	Length (mm)	Width (mm)
Reflector	29.184	42.440
Driven Patch	22.899	32.540
Director	20.064	29.040

After simulating the antenna with the new adjusted dimensions, the input reflection coefficient is shown in figure 2.12 and compared to the previous obtained results. The figure shows that the adjusted dimensions yield good result of the input reflection coefficient.

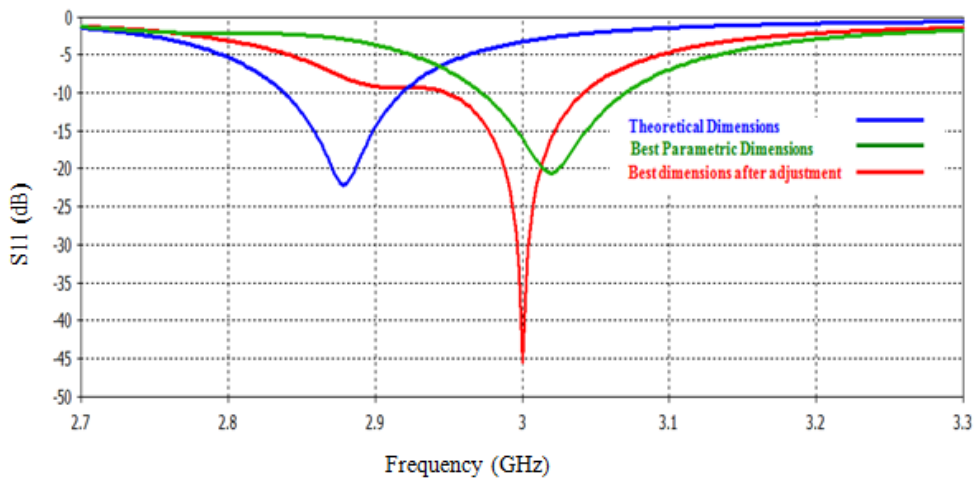


**Figure 2.12** Reflection Coefficient of the conventional planar Yagi antenna

## 2.6 Radio-Electric Properties of the Yagi-Uda Antenna

### 2.6.1 Input Impedance

In this section, the Yagi-Uda structure with the dimensions given table 2.4 is simulated. The obtained input impedance versus frequency is shown in figure 2.13. This figure shows the resonant behavior of the structure. The antenna presents an impedance of a real part of  $50 \Omega$  and an imaginary part is zero at the frequency of 3 GHz.

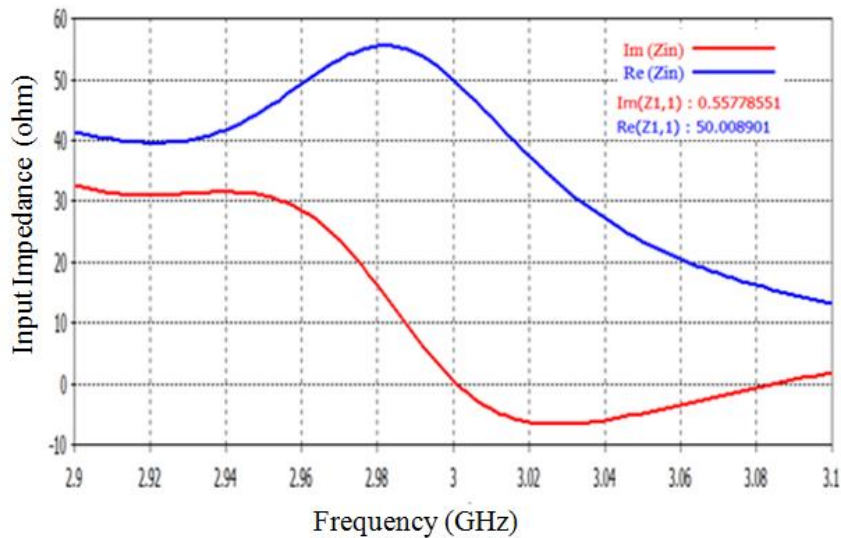


**Figure 2.13** Input Impedance versus frequency of the Yagi microstrip Antenna with best dimensions

### 2.6.2 Input Reflection Coefficient

The obtained reflection coefficient of the considered Yagi-Uda antenna is illustrated in figure 2.14. Since best dimensions are used, the antenna is resonating at the desired frequency with the magnitude of the input reflection coefficient at resonance of about  $-45\text{dB}$  which is much less than the  $-10\text{ dB}$  matching value.

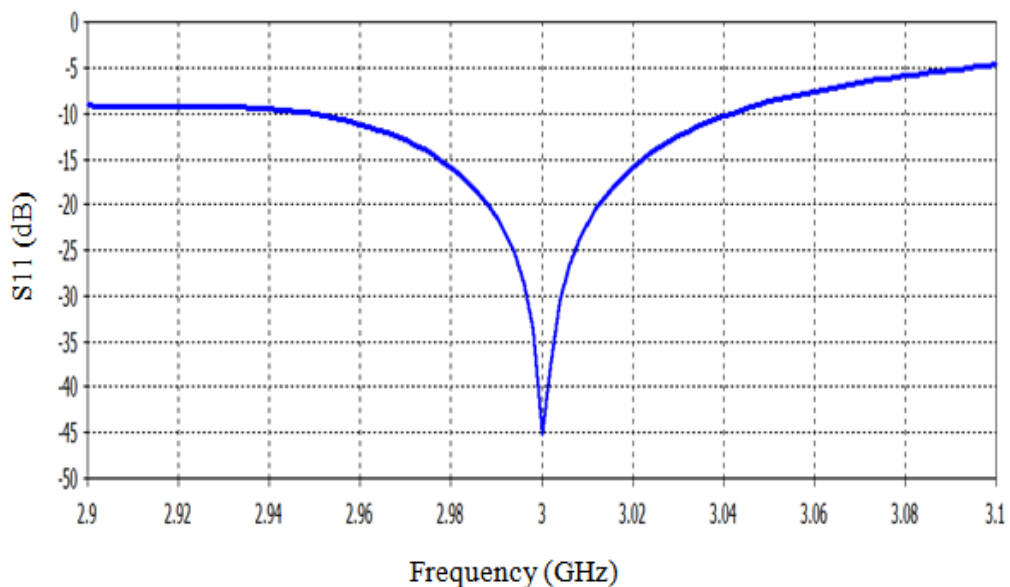


**Figure 2.14** Reflection Coefficient of the conventional planar Yagi antenna with the best dimensions

### 2.6.3 Bandwidth

The bandwidth is calculated from the input reflection coefficient graph in figure 2.14 evaluated to -10 dB using equation 1.4 as:

$$BW = \frac{3.0417 - 2.9488}{3} \times 100 = 3.096\%$$

This value indicates that the structure has narrow bandwidth. The bandwidth may be increased by decreasing the separation between the patches or by using the radiating edges instead of non-radiating edges.

### 2.6.4 Current Distribution

The current distribution is drawn at the frequency of 3 GHz as shown in figure 2.15. We can observe that the current is maximum in the center and around the feed port. Even though the parasitic patches are not fed, some current is distributed on them indicating the effect of mutual coupling between the patches elements. Mutual coupling refers to the electromagnetic interactions between the elements. Some of the energy transmitted by the driven patch is transferred to the other elements. The effect of the coupling between the patches elements is well illustrated in figure 2.15

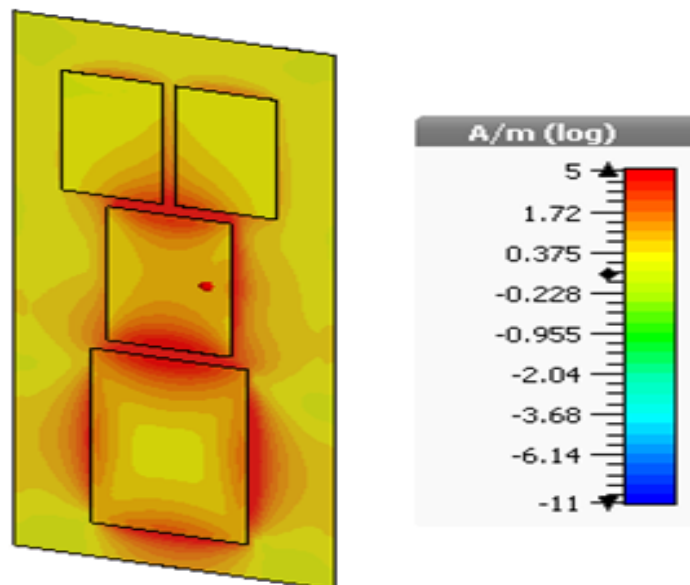


**Figure 2.15** Current distribution of the conventional Yagi antenna with the best dimensions at 3 GHz

### 2.6.5 Radiation Pattern

Far field pattern of the radiating antenna can be drawn. In the direction perpendicular to the ground plane the components of the field add in phase and give maximum radiation normal to the patch. Thus the antenna is a broadside one. Figure 2.16 shows the 3D representation of the radiation pattern at 3 GHz. It clearly shows that the printed Yagi-Uda antenna is a directional broadside radiating.

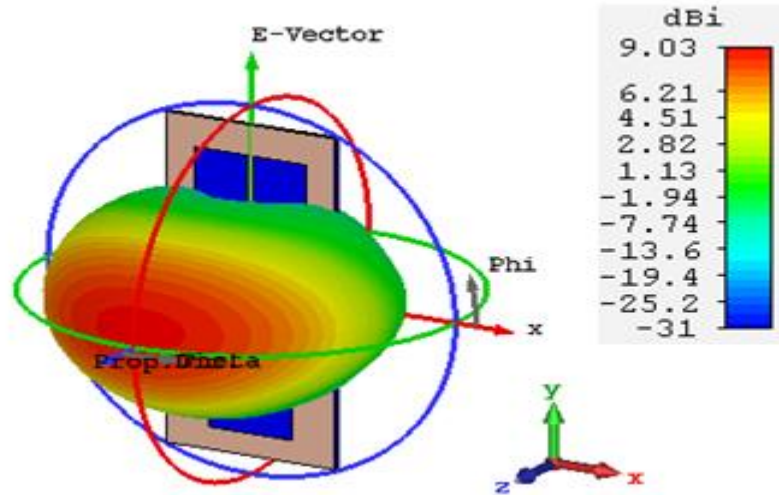


Figure 2.16 3D view of the Radiation Pattern at 3 GHz

The 2-D representation of the far field patterns, are shown in Figures 2.17 and 2.18. Since the excitation point is on the  $x$ -axis, the antenna is  $x$ -polarized (polarized along the  $x$ -axis).

The corresponding parasitic components are given as: 
$$\begin{bmatrix} E_{co} \\ E_{cross} \end{bmatrix} = \begin{bmatrix} +\cos\phi & -\sin\phi \\ +\sin\phi & +\cos\phi \end{bmatrix} \begin{bmatrix} E_{\theta} \\ E_{\phi} \end{bmatrix}$$

For  $\phi = 0^\circ$  (E-plane):  $\begin{cases} E_{co} = E_{\theta} \\ E_{cross} = E_{\phi} \end{cases}$  and for  $\phi = 90^\circ$  (H-plane):  $\begin{cases} E_{co} = -E_{\phi} \\ E_{cross} = E_{\theta} \end{cases}$

To study the polarization purity, both co-polar and cross-polar components of the radiated field are drawn in the E-plane and H-plane. The graphs are shown below in figure 2.17 and figure 2.18.

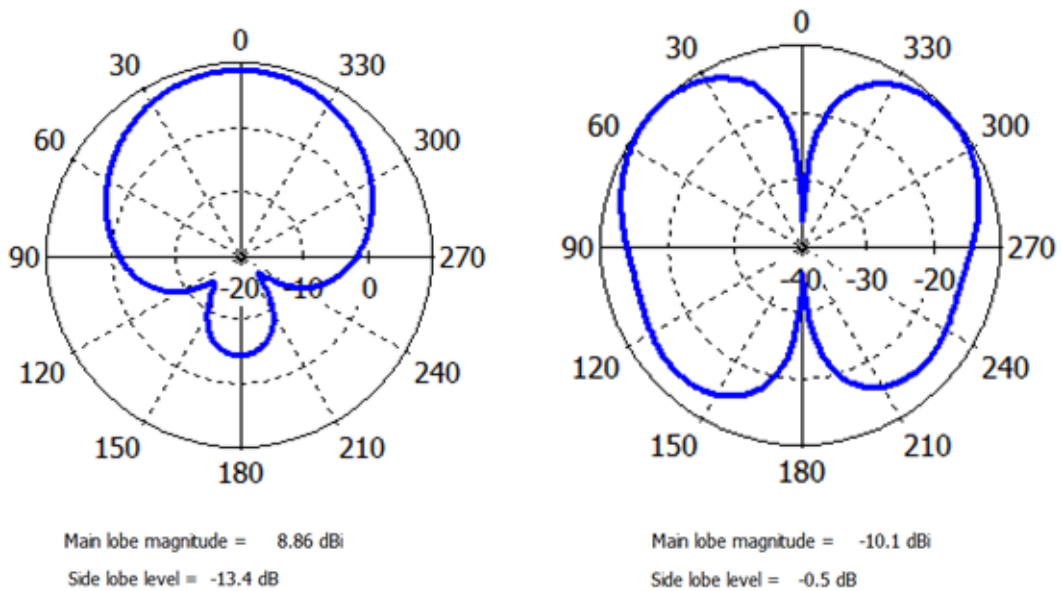
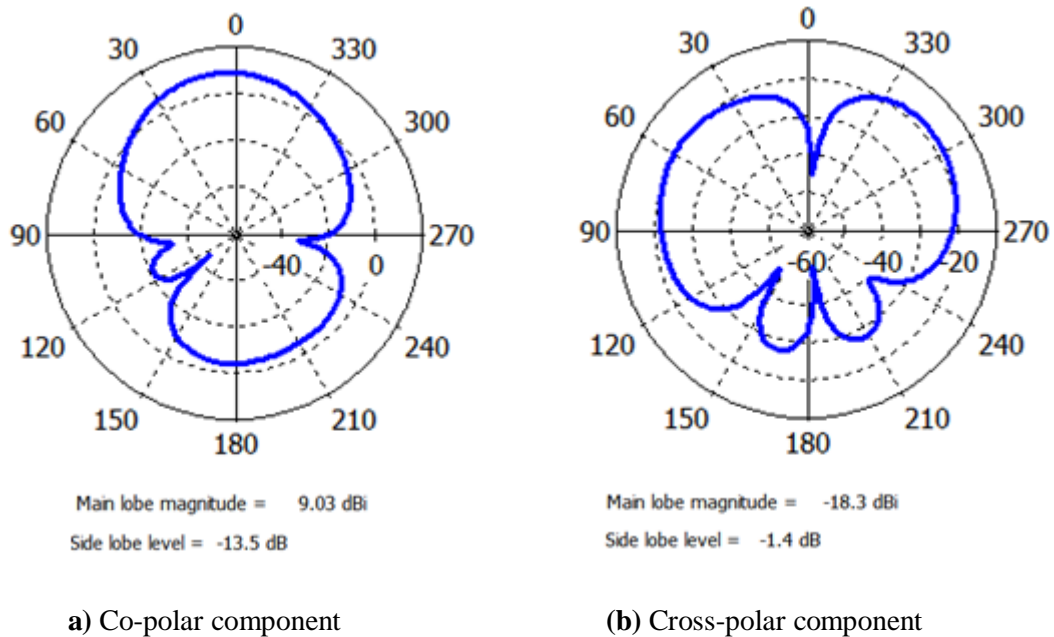


Figure .17 E-plane radiation pattern of the conventional Yagi antenna with the best dimensions at 3 GHz



**Figure 2.18** H-plane radiation pattern of the conventional Yagi antenna with the best dimensions at 3 GHz

According to the above figures, the radiation characteristics of microstrip antenna structures gradually decrease to zero at  $\pm 90^\circ$ ; with a back lobe of about -21.53 dB below the main lobe. From the figure we notice that the level of the cross-polarization components, noted  $E_{cross}$ , are -18.96dB (greater than the conventional value) lower than the co-polar components the E-plane and -27.33 dB lower than the co-polar components in H-plane indicating that the antenna has good polarization purity.

**Table 2.5** Far field zone Characteristics

Cutting plane	Main lobe direction	-3 dB angles	Beamwidth width	Front to back ratio
E plane	0°	43.9°, 317.4°	86.5°	22.26 dB
H plane	6°	28.8°, 341.5°	47.4°	22.53 dB

Table 2.5 demonstrates the far field zone characteristics where the -3dB beam-width in the E- and H-planes are 86.5° and 47.4°, respectively. This yields a directivity of 9.03dB besides that the antenna has a high front to back ratio which is about 22dB

### 2.7 Conclusion

In this chapter, the proposed Yagi-Uda microstrip patch antenna is designed and the effect of its different dimensions is investigated. Adjustment on the antenna dimensions has been performed to achieve the desired resonant frequency. The designed antenna efficiently resonates around 3GHz frequency and gives good return loss, with an impedance matching of 50Ω and presents a high directional broadside radiation pattern and high front to back ratio

# CHAPTER 3

---

*Design and Analysis of a Miniaturized Yagi-Uda  
Microstrip Patch Antenna*

## Chapter 03: Design and Analysis of a Miniaturized Yagi-Uda Microstrip Patch Antenna

### 3.1 Introduction

In this chapter, the design and the analysis of a miniaturized Yagi-Uda microstrip patch antenna is presented. The miniaturization is based on the use of defected microstrip structure technique. The proposed slot geometry is introduced as DMS and its effect on the antenna properties is studied. Next a comparison between the miniaturized Yagi-Uda antenna and the conventional antenna presented in the previous chapter is illustrated. Finally both the conventional and miniaturized antennas are fabricated and measured to validate the proposed designs

### 3.2 Defect Geometry and Dimensions

To see the effect of the introduced defect, the dielectric material and the patch elements dimensions are unchanged. The introduced defect, as illustrated in Figure 3.1.a, has dimensions:  $l_1 = 6\text{mm}$ ,  $l_2 = 4\text{mm}$  and  $t = 1\text{mm}$ . We named the proposed slot as ‘‘Vase slot’’. It is inserted in all the elements of the printed Yagi-Uda antenna as shown in Figure 3.1.b. It is informed that the used slot dimensions are chosen after several simulations.

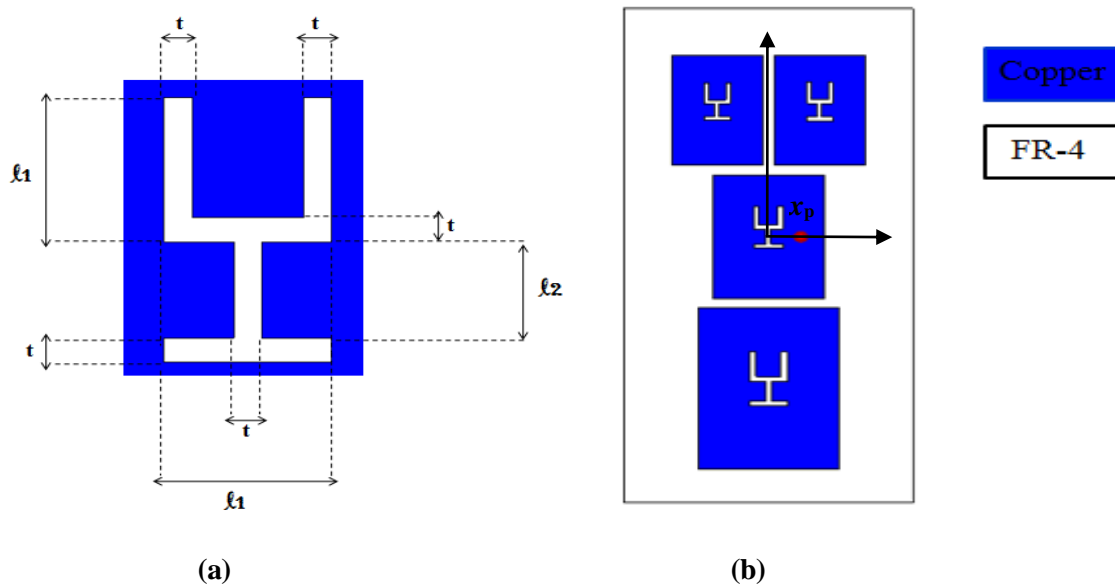


**Figure 3.1** (a) The Vase Slot Dimensions, (b) Front View of the defected printed yagi antenna

### 3.3 Simulations Results and Discussion

#### 3.3.1 Input Impedance

First the proposed structure is simulated for the input impedance. The obtained variation of this parameter versus frequency is illustrated in Figure 3.2 where it can be clearly seen that the structure keeps the resonant behavior except the resonant frequency is shifted down as expected based on the theory of chapter 1. The obtained resonant frequency has shifted from 3 GHz to 2.682 GHz; which reveals the possibility of the size reduction since the resonant frequency is inversely proportional to the patch resonant length.

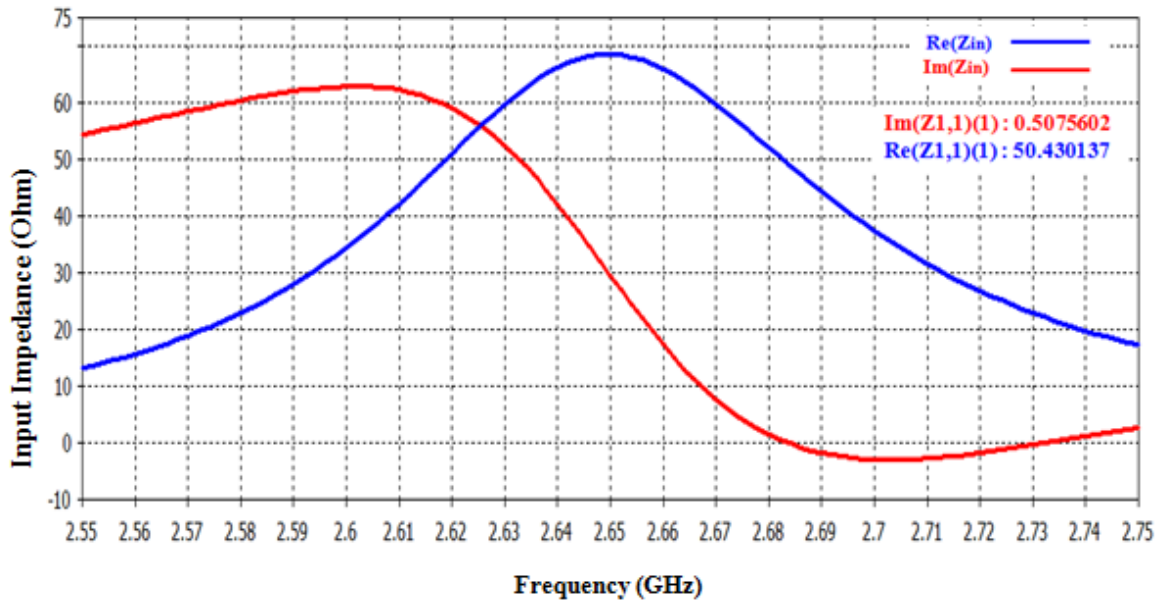


Figure 3.2 Input impedance versus frequency of the defected printed Yagi-Uda antenna

### 3.3.2 Input Reflection Coefficient

The obtained reflection coefficient of the considered defected Yagi-Uda antenna is illustrated in Figure 3.3. It can be observed that in introduction of the Vase DMS, the resonant frequency is shifted from 3 GHz to 2.682 GHz with the magnitude of the input reflection coefficient about -44 dB. It should be noted that this result is obtained after modifying the feeding point ( $X_p$  is moved from 6.7 mm to 2.7 mm). But, this modification affected only impedance levels without resonant frequency.

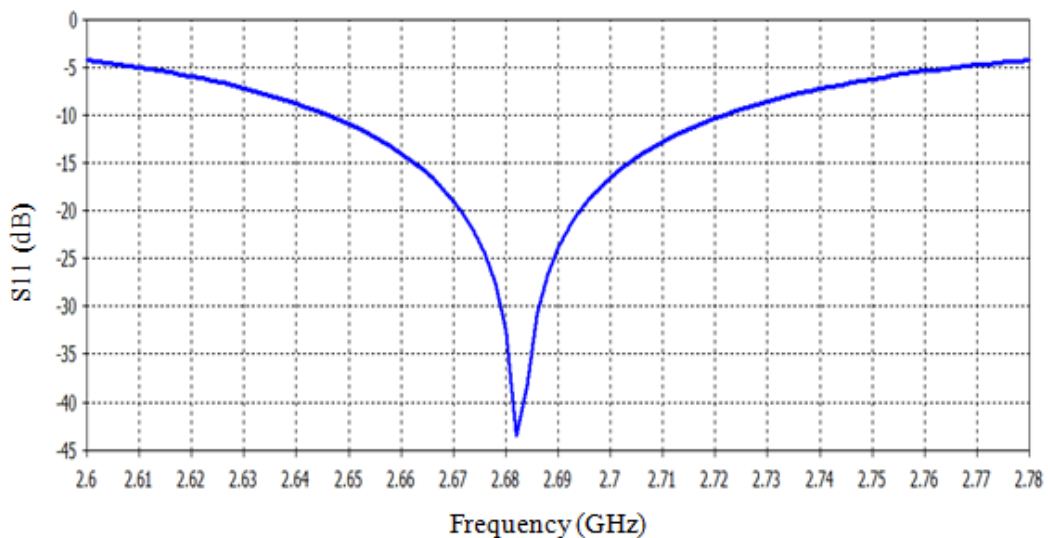


Figure 3.3 Input reflection coefficient of the defected printed Yagi-Uda antenna

### 3.4 Results of the Reduced Size Printed Yagi-Uda Antenna

In order to recuperate the resonance frequency of the antenna structure to the desired frequency, 3 GHz, the size of its dimensions must be reduced. To this end, using the method of cut and try; the new structure dimensions are summarized in table 3.1.

**Table 3.1** Dimensions of the miniaturized Yagi-Uda antenna

Elements	Length (mm)	Width (mm)
Reflector	24.89	28.8
Driven Patch	19.88	29.9
Director	15.3	20.3

#### 3.4.1 Input Impedance

Figure 3.4 shows the input impedance versus frequency of the reduced size of the defected Yagi-Uda antenna. It is clearly seen that the original resonant frequency 3GHz is recovered. Also, at that frequency the antenna presents impedance with real part of around 50  $\Omega$  and an imaginary part around null. Of course this result is obtained after feeding the antenna at the point (1.5 mm, 0mm).

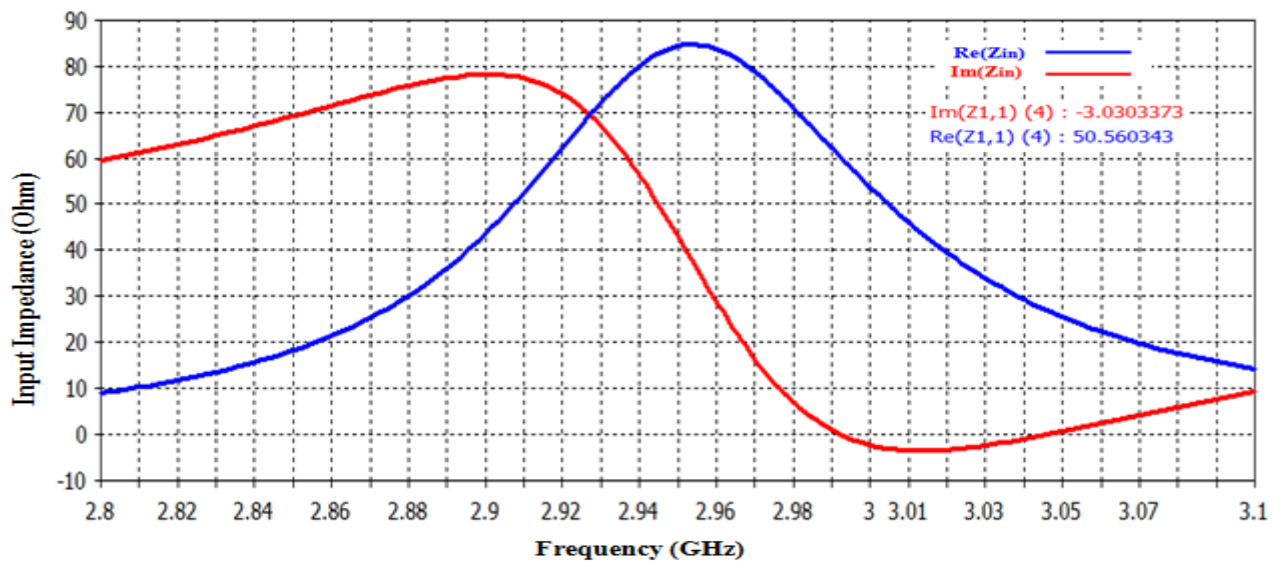


**Figure 3.4** Input impedance of the reduced radiating structure

#### 3.4.2 Input Reflection Coefficient

The simulated reflection coefficient of the reduced size Yagi-Uda antenna is shown in Figure 3.5. It can be observed that the antenna is resonating at the desired frequency with the magnitude of the input reflection coefficient at resonance of about -30 dB which is much less than the -10 dB matching value. Using the formula, (1.3), the -10 dB bandwidth is about 2.9%, which remained almost unchanged as compared to the conventional Yagi-Uda antenna.

$$BW = \frac{3.0487 - 2.9611}{3.004} \times 100 = 2.916\%$$

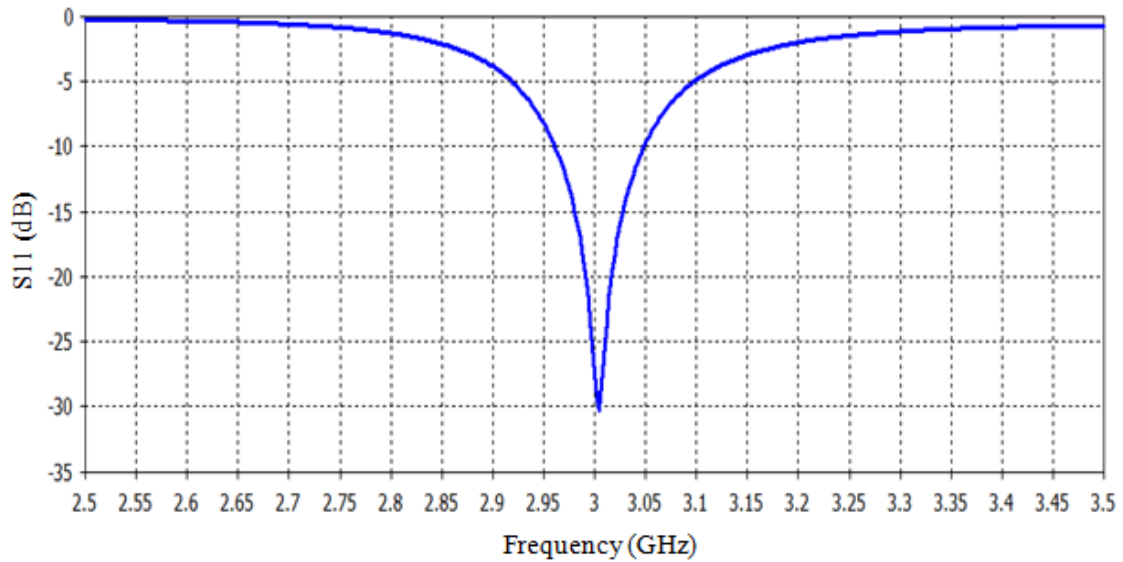


**Figure 3.5** Input reflection coefficient of the reduced size Yagi-Uda structure

### 3.4.3 Current Distribution

The current distribution is drawn at the frequency of 3 GHz as shown in figure 3.6. We can observe that by introducing the defect, the current distribution on the patch is altered leading to longer current path.

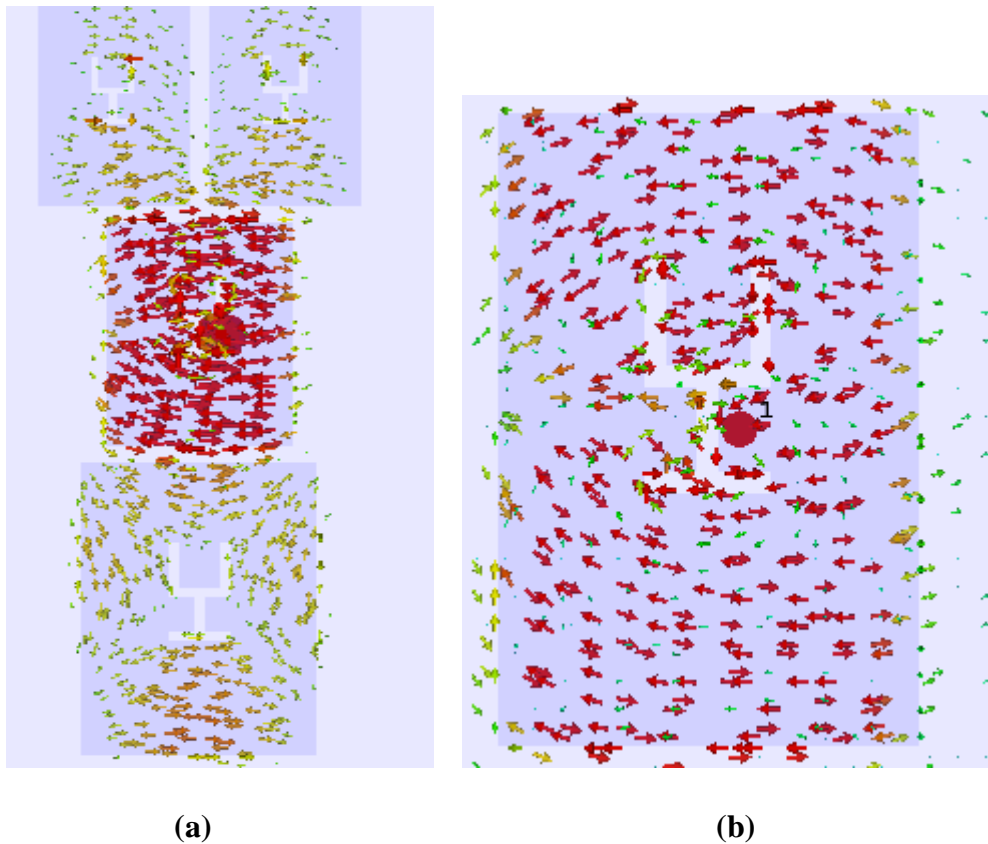


**Figure 3.6** (a) The current distribution of the defected printed Yagi antenna (b) The current distribution of the defected Pilot element of the printed Yagi antenna

**3.4.4 Radiation Pattern**

The 2-D radiation pattern of the reduced size antenna is drawn in Figure 3.7 and figure 3.8 for both co-polar and cross-polar and in both E- and H- planes. The obtained fields show clearly that neither the form of the pattern nor the maximum radiation direction is affected. In addition, the introduction of the Vase slot has lead to an improvement of the polarization purity especially in the E-plane. Quantitatively, the level of the cross polar components in both planes is lower than -22 dB

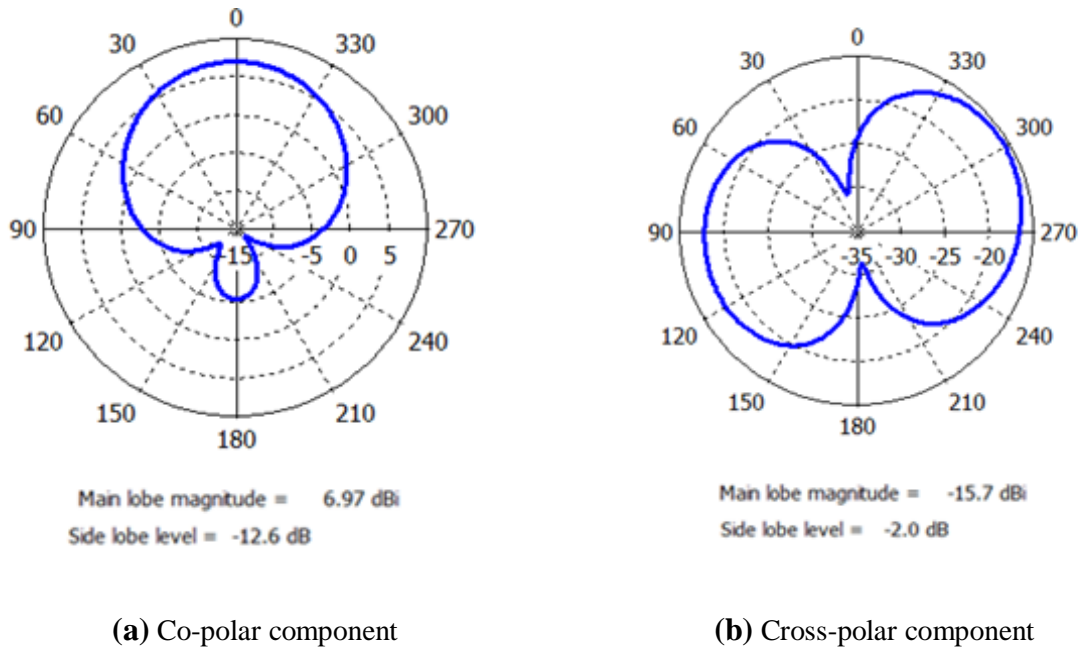


**Figure 3.7** E-plane radiation pattern of the miniaturized yagi-uda antenna at 3 GHz

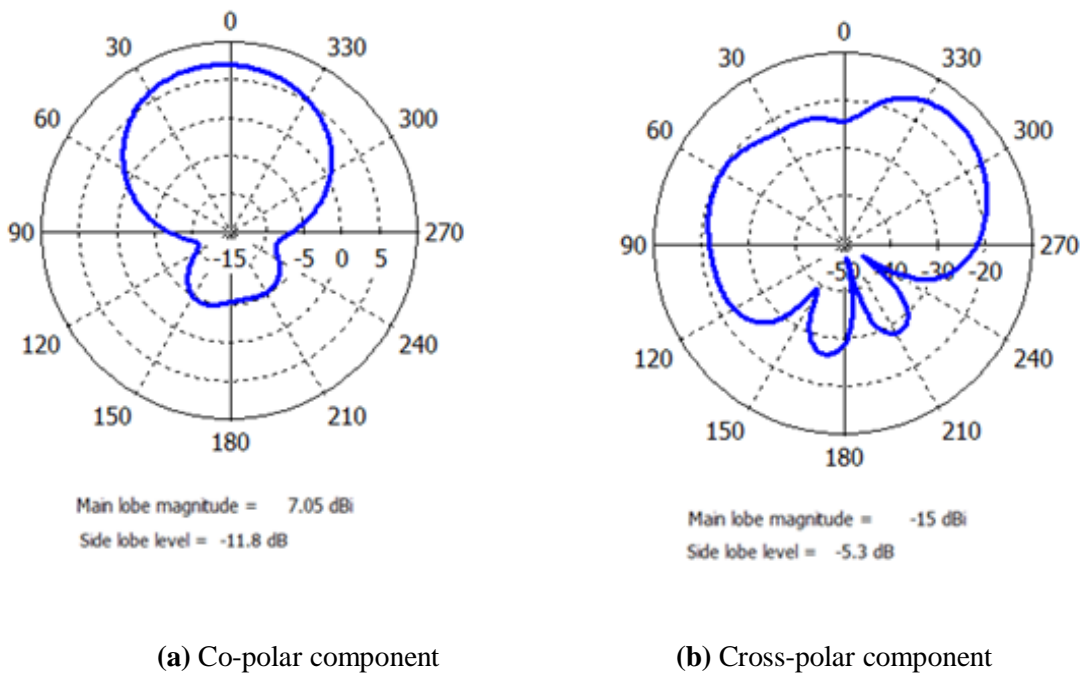


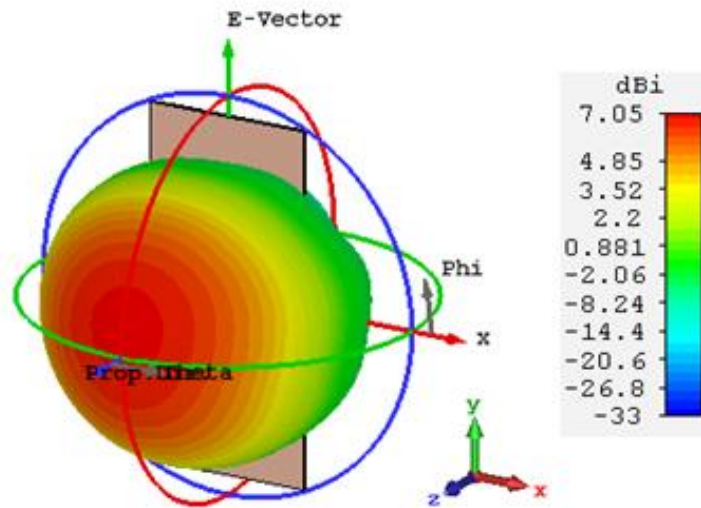
**Figure 3.8** H-plane radiation pattern of the miniaturized Yagi-Uda antenna at 3 GHz

**Table 3.2** Far field zone characteristics

Cutting plane	Main lobe direction	-3 dB angles	Beamwidth width	Front to back ratio
E plane	0°	44.55°, 316.9°	87.7°	19.57 dB
H plane	8°	46.2°, 320.3°	85.8°	18.85 dB

According to the table 3.2, the  $-3\text{dB}$  beam-width in the E- and H-planes are  $87.7^\circ$  and  $85.5^\circ$ , respectively. This yields a directivity of  $7.05\text{dB}$  and a high front to back ratio of about  $19\text{dB}$  which is suitable for applications where the backside level needs to be suppressed; these values indicate that the miniaturization preserved the good performance of the Yagi-Uda antenna

To have a general view of the radiation properties of the Yagi-Uda antenna, the 3-dimensional power pattern is also illustrated in figure 3.9. The figure indicates the broadside radiation nature of the structure.

**Figure 3.9** 3D view of the Radiation Pattern at 3 GHz

### 3.4.5 Comparison between the Conventional and Miniaturized Yagi-Uda Antenna

Figure 3.10 shows the structures of both the conventional and the reduced size Yagi-Uda antenna with the patch dimensions summarized in table 3.3. This comparison is quantified by calculating the surface size reduction. The calculation of the surface is carried out by concentrating on metallic surface by considering a rectangle of the length and width of  $L_p$  and  $W_p$  for each structure. The obtained result is:

$$\text{Surface size reduction} = \frac{4647.305 - 2780.400}{4647.305} \times 100\% = 40.17\%$$

Therefore, the Vase Slot leads to a surface size reduction of about 40% compared with the conventional antenna designed in the second chapter.

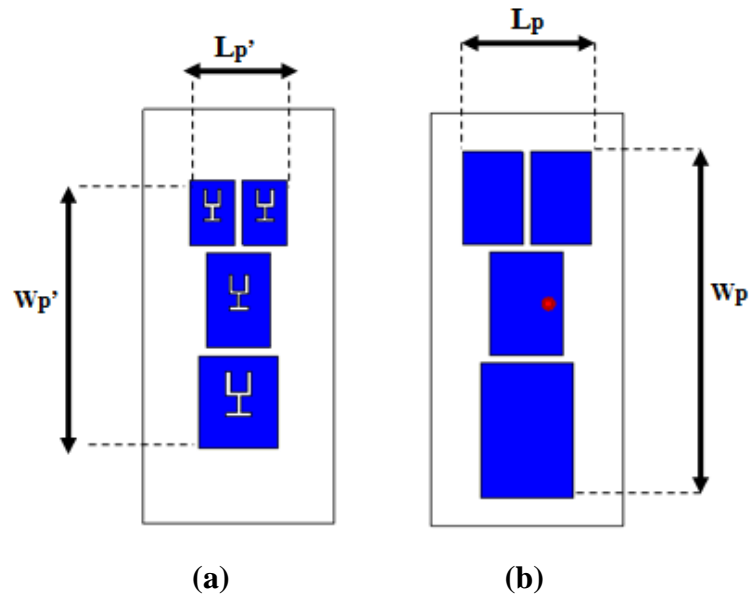


**Figure 3.10** (a) Miniaturized Yagi-Uda antenna, (b) Conventional Yagi-Uda antenna

**Table 3.3** Dimensions of the miniaturized antenna

Antenna dimensions	Length (mm)	Width (mm)	Surface (mm <sup>2</sup> )
conventional yagi-uda antenna	42.628	109.02	4647.305
miniaturized yagi-uda antenna	33.100	84.00	2780.400

The performances of the previous structures are summarized in table 3.4 in terms of the directivity and the gain.

**Table 3.4** Summary of the obtained results

Structure	Resonance frequency (GHz)	Directivity (dBi)	Gain (dBi)
The rectangular patch antenna	3.000	6.67	4
The miniaturized rectangular patch antenna	2.997	6.63	3
The conventional printed Yagi antenna	3.000	9.03	4.84
The miniaturized printed Yagi antenna	3.004	7.05	3.34

It may be seen from the above results that when the concepts of Yagi-Uda dipole antenna and a Microstrip patch antenna are interlinked, a much high performance antenna is obtained in terms of gain, directivity and front to back ratio as compared to the isolated rectangular patch antenna.

In the case of the isolated rectangular patch antenna miniaturization can be achieved at the cost of the gain; while the radio-electric properties are not affected. In the case of the Yagi

antenna, miniaturization also leads to a reduction in the gain and directivity by 2dB but there is an increase as compared to a reduced size isolated rectangular patch.

The introduction of the Vase slot in all Yagi elements used for miniaturization in our work is compared to the work done in [1]. In that work, the metamaterial structures are incorporated in the antenna in place of directors. This technique has yielded a directivity of 6.28dB and a size miniaturization of 33.3% is achieved. However, our work has yielded a directivity of 7.05dB and size reduction of 40%.

### 3.5.1 Realization of the Yagi-Uda Antennas

In this section the designed antennas in the previous chapters are fabricated and their input reflection coefficients are measured using the vector network analyzer available in the telecommunication laboratory. The antennas are constructed from the double sided FR4 as substrate material; the obtained structures are shown in figure 3.11



**Figure 3.11** Front and back views of the realized Yagi-Uda antennas with and without slots

### 3.5.2 Measurements of the Fabricated Yagi-Uda Antennas

Using the vector network analyzer, shown in the figure 3.12, the input S-parameters,  $S_{11}$ , of both the fabricated conventional and miniaturized Yagi-Uda patch antennas are measured. The magnitude of the input reflection coefficients in dB and its phase angles are taken in a file versus frequency around 3 GHz.



Figure 3.12 Vector network analyzer used for  $S_{11}$  measurement

The Origin-Pro software is used to plot the measured input reflection coefficient along with the simulated results which are shown in figures 3.13 and 3.14 respectively.

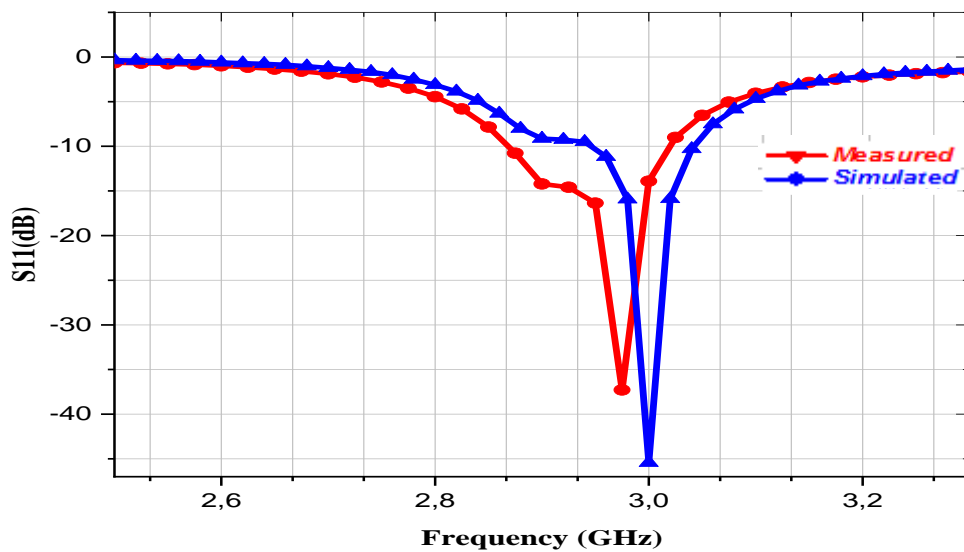


Figure 3.13 The input reflection coefficient of the fabricated conventional Yagi antenna

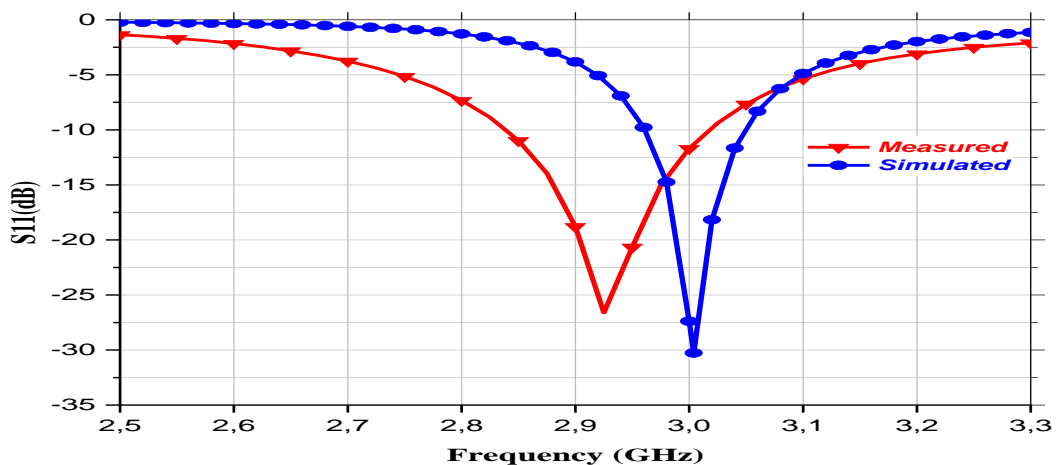


Figure 3.14 The input reflection coefficient of the fabricated miniaturized Yagi antenna

The quantitative results of the comparison between measured and simulated parameters are summarized in tables 3.5

**Table 3.5** comparison between the simulated and measured parameter

Parameters		Resonant frequency $f_r$ (GHz)	Input reflection coefficient in dB	Percentage measurement error	Bandwidth
conventional Yagi-Uda antenna	Simulated	3	-44	15.22%	%3.
	Measured	2.975	-37.3		5.04%
miniaturized Yagi-Uda antenna	Simulated	3.004	-30	11.3%	%2.9
	Measured	2.925	-26.61		5.9%

From table 3.5, both the fabricated conventional and miniaturized Yagi-Uda antennas resonate around the wanted frequency, their input return loss has a level of -37.3dB and -26.6% respectively. The slight difference between the two measured and the simulated results present errors of around 15% and 11% respectively.

The comparison between the measured and the simulated results shows acceptable level of agreement but with a small deviations in the frequency and the level of return loss; this is due to the following reasons:

- The dielectric material used in the fabrication may have a relative permittivity  $\epsilon_r$  different from the one used in simulation
- The measurement environment which contains the reflecting objects.
- Tolerance in fabrication and Soldering.
- The SMA connector used in the fabrication has a diameter of **1.3 mm** whereas the one used in the simulation was **1 mm**; which leads slight change in the excitation point position.

### 3.6 Conclusion

This chapter covers the design and analysis of a reduced size Yagi-Uda microstrip patch antenna. The Vase slot is introduced as DMS and its effect on the antenna performance and the resonance frequency is investigated. Next a comparison between the miniaturized Yagi-Uda antenna and the conventional antenna is presented. Where a surface size reduction of 40% is achieved; finally both the conventional and miniaturized Yagi antennas are fabricated and measured. The two realized antennas efficiently resonates around the desired frequency and gives good return loss.

## General Conclusion and Further Work

In this report, the Yagi-Uda patch antenna is designed to resonate at 3 GHz, RADAR frequency. The design (initial values) is carried out based on the empirical formulae that exist in literature. The patch dimensions have been calculated and refined using simulations based on CST microwave studio software. The excitation point is fixed at a specific location giving  $50 \Omega$  at the 3 GHz. The near zone properties as well as far zone have been obtained. The designed antenna presents an increased directivity as compared to the isolated rectangular patch, front to back ratio and a low level of cross-polarization that are essential parameters for the design of planar antennas with linear polarizations.

The work is extended to the design and analysis of a miniaturized Yagi-Uda microstrip patch antenna. The miniaturization is based on the use of defected microstrip structure technique. The defect has a new shape named '*Vase*'. The obtained results show that, both conventional and miniaturized antennas are resonant and narrow in bandwidth. Further, the Yagi antennas radiate linear waves in broadside direction without secondary lobes. Next, a comparison between the miniaturized Yagi-Uda antenna and the conventional antenna and also to the isolated rectangular patch antenna is illustrated.

The designed antennas are fabricated and tested. The comparison with the simulations confirms the exactitude of the design. The measured result shows an acceptable extent of agreement with the simulated ones. The small noticed deviations are attributed to the environment and the substrate used that requires an identification of its physical properties before its use. As further work, we may propose the following tasks:

- Design this antenna at other commercial frequencies such as WIFI and Bluetooth.
- Implement the antenna with better substrate material and with the appropriate SMA connector.
- Design the Yagi antenna with the parasitic connected in the radiating edges.
- Design the Yagi antenna with circular polarization.
- Use of other technique for size reduction such as DGS and Fractals.
- Increase the bandwidth of the antenna by using metamaterial.

# References

---

# References

- [1] Rhitam Datta, Tarakeswar Shaw, and Debasis Mitra; “Miniaturization of Microstrip Yagi Array Antenna Using Metamaterial” Progress In Electromagnetics Research C, Vol. 72, 151–158, 2017
- [2] Constantine A. Balanis, “Antenna theory, analysis and design”, third edition, Hoboken, NJ: Wiley, 2005, ISBN 047166782X
- [3] Prasanna Ramachandran, T.S.Keshav, Laxmikant Minz, “Antenna design, simulation and fabrication”, Department of Electronics and Computer Science Engineering Visvesvaraya National Institute of Technology (2006-2007)
- [4] A. Azrar, “Course Handout of Antennas”, destined for M01 Telecommunication-option students, Institute of Electrical and Electronic Engineering, university of Boumerdes, Algeria
- [5] Yi Huang, Kevin Boyle “Antennas from theory to practice”, John Wiley & Sons Ltd, 2008, ISBN 978-0-470-51028-5
- [6] Pristin K Mathew, “A Three Element Yagi Uda Antenna for RFID Systems”, 2014 IJEDR Volume 2, and Issue 1 | ISSN: 2321-9939
- [7] [http://dewan.buet.ac.bd/EEE433/CourseMaterials/YagiUda\\_Antenna.pdf](http://dewan.buet.ac.bd/EEE433/CourseMaterials/YagiUda_Antenna.pdf)
- [8] <https://www.electronics-notes.com/articles/antennas-propagation/yagi-uda-antenna-aerial/gain-directivity.php>.
- [9] Hamrioui Fatma Zohra; Bouhafis Djazia, “Gain Enhancement of Microstrip Antenna Using Artificial Magnetic Conductor” Master Thesis, IEEE/ University M’Hamed BOUGARA, Boumerdes, 2020.
- [10] B. D. Patel, “Microstrip Patch Antenna- A Historical Perspective of the Development”, H. O. D, E. T Department, College Of Engineering Roorkee, Roorkee, U.A-247667, India.
- [11] Densmore, A. and J. Huang, “Microstrip Yagi antenna for mobile satellite service,” IEEE Transactions on antennas and propagation, VOL 39, No 7, July 1991.
- [12] J.Huang, “Planar microstrip Yagi array antenna,” IEEE Antennas and Propagation Society, Vol. 2, 894-897, Jun. 1989.
- [13] Shivani Chourasia, Dr Sudhir Kumar Sharma, Dr Pankaj Goswami “Review on Miniaturization Techniques of Microstrip Patch Antenna”, International Conference on Innovative Advancement in Engineering and Technology (IAET-2020).
- [14] JIAN-KANG XIAO Xidian University. Webster (ed.), Wiley Encyclopedia of Electrical and Electronics Engineering. Copyright © 2013 John Wiley & Sons, Inc.

- [15] Elftouh Hanae, Naima Amar Touhami, and Mohamed Aghoutane. “Miniaturized microstrippatch antenna with spiral defected microstrip structure”. *Progress in Electromagnetics Research*, 53:37\_44, 2015.
- [16] Himanshu Patel, Shobhit K. Patel, Jaymin Bhalani and Y. Kosta Design of Meandered H-Shaped Square Microstrip Patch Antenna.
- [17] Vivek Singh Kushwah, Geetam Singh Tomar “Size reduction of Microstrip Patch Antenna using Defected Microstrip Structures”, 2011 International Conference on Communication Systems and Network Technologies.

# Appendix

---

# Appendix A: Introduction To CST Microwave Studio

CST MWS is an efficient tool for 3D EM simulation enabling high accuracy simulation results for complex antenna structures and it specifically suitable for wideband antenna simulation. It has a much better interface which enables the user to include very fine details in the geometry of the simulated structure. This software offers a number of different solvers, mainly time and frequency domain for its high accuracy, and that's for different types of application in a very high frequency range. The figure A.1 shows the different application the in CST software.

Create Project Template

Choose an application area and then select one of the workflows:

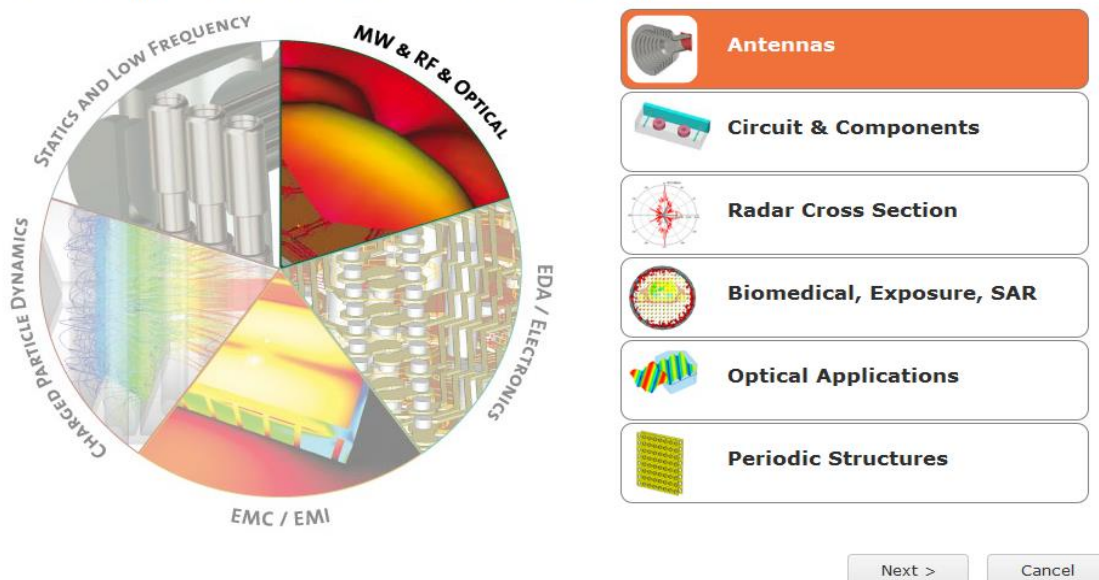


**Figure A.1:** Front page of CST showing the different application available.

This software is used to design all components which belong to our antenna system. It is a specialist tool for the 3D Electromagnetic (EM) simulations of high frequency components. It includes multi signal functionality to simulate various excitations. Has the ability to calculate E-field patterns, far field, S-parameters, radiation efficiency and total radiation efficiency besides many antenna parameters by using powerful different kind of solvers such as Time domain solver, Frequency domain solver, and Transient solver. It allows mesh generation that divided the system to small cells in order to get accurate results.

In order to create a patch antenna project the following steps are needed:

- After launching the CST simulator with a double click, create a new project “New Template”. You will be prompted to select “MW & RF & OPTICAL” (Figure A.1).

- After choosing "Antennas", Next → "Planar" as shown in figure A.2.
- Then you click on next → Time Domain as illustrated in figure A.3.
- Choose the parameters that defines the units of the dimensions, frequencies, time and temperature, etc (Figure A.4)
- After that select the minimum and maximum frequency and simulation field as depicted in figure A.5.
- After reviewing the choice and by clicking finish as demonstrated in figure A.6; the template where the design, modeling and simulation of the antenna structure is shown in figure A.7.

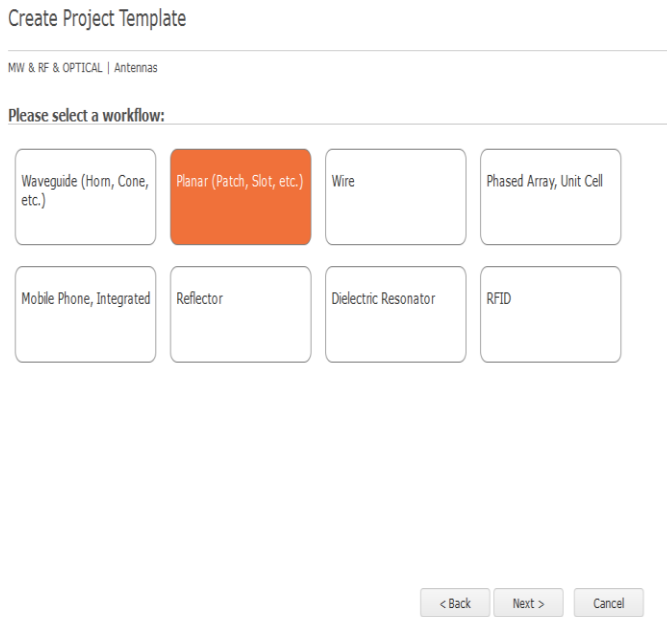


Figure A.2

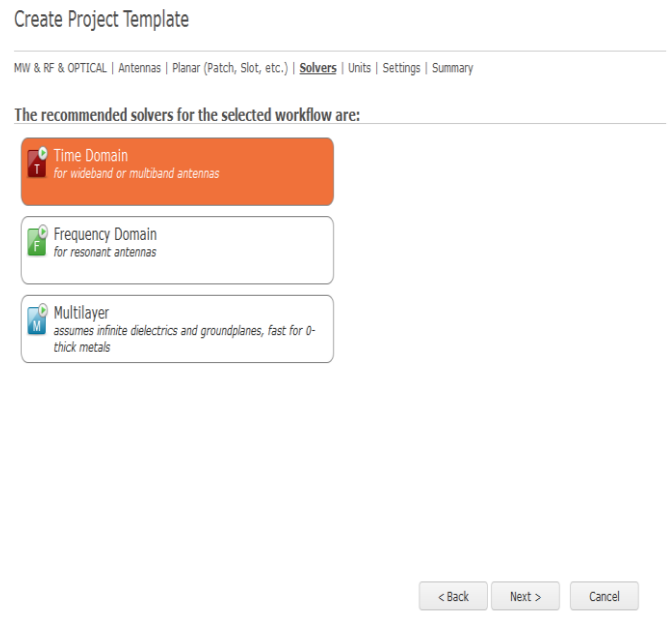


Figure A.3

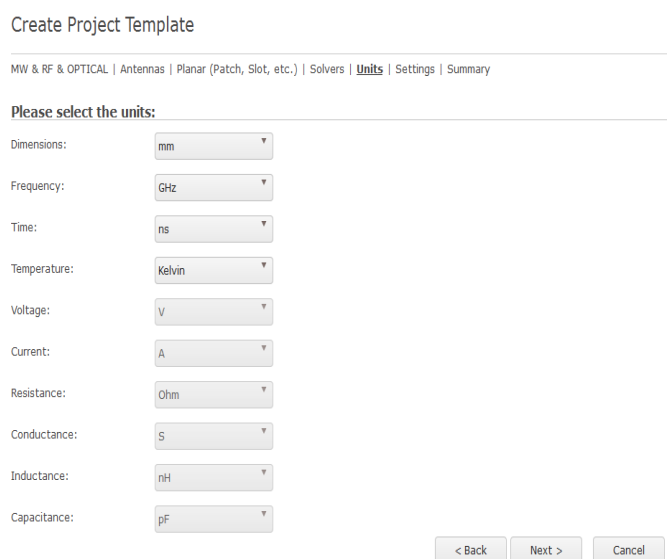


Figure A.4

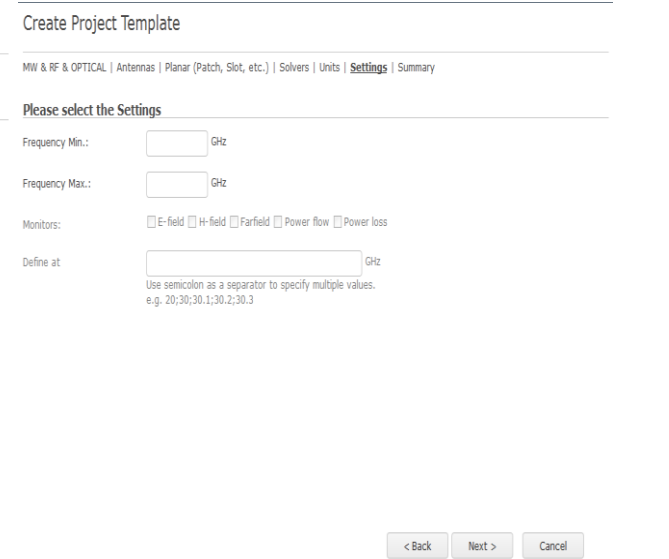
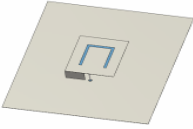



Figure A.5

Please review your choice and click 'Finish' to create the template:

Template Name:



**Solver**



Time Domain

**Units**

- Dimensions: mm
- Frequency: GHz
- Time: ns
- Temperature: Kelvin

**Settings**

- Undefined

Antennas which consist of flat radiating elements, e.g. printed microstrip, PIFA, slot, spiral or monopole geometries.

Figure A.6

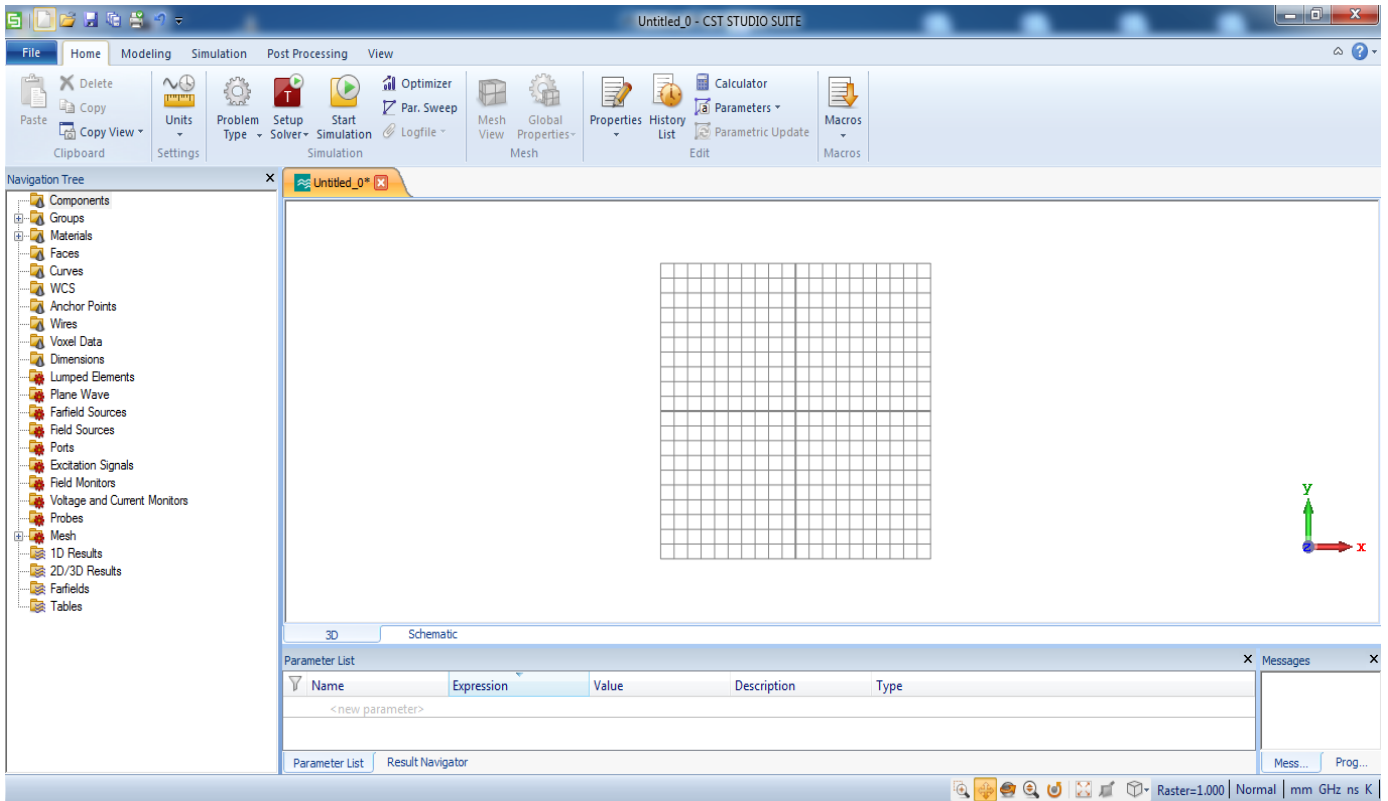


Figure A.7